A Late Pliocene *Hipparion houfenense* fauna from Yegou, Nihewan Basin and its biostratigraphic significance

LIU Jin-Yi[1,2] ZHANG Ying-Qi[1,2] CHI Zhen-Qing[3] WANG Yong[3]
YANG Jin-Song[4] ZHENG Shao-Hua[1]

(1 *Key Laboratory of Vertebrate Evolution and Human Origins of Chinese Academy of Sciences*, *Institute of Vertebrate Paleontology and Paleoanthropology*, *Chinese Academy of Sciences* Beijing 100044 zhangyingqi@ivpp.ac.cn)
(2 *CAS Center for Excellence in Life and Paleoenvironment* Beijing 100044)
(3 *Institute of Geology*, *Chinese Academy of Geological Sciences* Beijing 100037)
(4 *Institute of Hydrogeology and Environmental Geology*, *Chinese Academy of Geological Sciences* Shijiazhuang 050061)

Abstract Currently, there are still different views regarding the chronology of the Late Cenozoic deposits in the Nihewan Basin, which results from the contradiction between biostratigraphic correlations based on mammalian fossils and magnetostratigraphic dating results. Biostratigraphic correlations indicate that the aeolian red clay exposed in the Sanggan River canyon, the fluvio-lacustrine red clay with sands and gravels, and the sandy clay of swamp facies on both sides of the lower reaches of the Huliu River belong to the Upper Pliocene, whereas the magnetostratigraphic dating usually correlates them to the Lower Pleistocene. In October 2011, a collection of mammalian fossils was unearthed from a block of collapsed deposits at Yegou in the Nihewan Basin, which is about 300 m north of the Laowogou section that is well known for the Pliocene mammalian fossils from its lower part. The Yegou fossils are identified herein as 10 species in 9 genera: *Nyctereutes tingi*, *N. sinensis*, *Pachycrocuta pyrenaica*, *Homotherium* sp., *Hipparion* (*Plesiohipparion*) *houfenense*, *Dicerorhinus* sp., *Muntiacus* sp., *Axis shansius*, *Gazella blacki*, and *Paracamelus* sp. The fauna is quite different from the classic Early Pleistocene Nihewan Fauna in composition and provides new evidence for the existence of the Upper Pliocene in the Nihewan Basin. Based on a systematic description of the fauna, its composition and geological age are discussed, and the compositional features of large mammals of the Late Pliocene and the Early Pleistocene mammalian faunas in the Nihewan Basin are summarized.

Key words Nihewan Basin, Upper Pliocene, large mammals, *Hipparion* (*Plesiohipparion*) *houfenense*, biostratigraphy, magnetostratigraphy

Citation Liu J Y, Zhang Y Q, Chi Z Q et al. in press. A Late Pliocene *Hipparion houfenense* fauna from Yegou, Nihewan Basin and its biostratigraphic significance. Vertebrata PalAsiatica.

中国科学院战略性先导科技专项(B类) (编号：XDB26000000)和国家自然科学基金(批准号：41772018)资助。
收稿日期：2021-07-02

1 Introduction

In 2011, CHI Zhen-Qing of Institute of Geology, Chinese Academy of Geological Sciences invited ZHENG Shao-Hua of Institute of Vertebrate Paleontology and Paleoanthropology, Chinese Academy of Sciences to carry out a joint investigation in the Nihewan Basin. On October 4th of that year, the team discovered abundant fossils of large mammals at Yegou, north of Daodi Village, which are identified herein as 10 species in 9 genera: *Nyctereutes tingi*, *N. sinensis*, *Pachycrocuta pyrenaica*, *Homotherium* sp., *Hipparion* (*Plesiohipparion*) *houfenense*, *Dicerorhinus* sp., *Muntiacus* sp., *Axis shansius*, *Gazella blacki*, and *Paracamelus* sp. The Yegou locality (N40°9′9.9″, E114°39′19.4″) is located about 300 m north of the Laowogou section, the stratotype of the "Daodi Formation" (Du et al., 1988). The fossils were unearthed from a big block of collapsed deposits, the lithology of which is dark brownish grey silty clay. However, the stratigraphic section is not exposed. Based on the fossils, lithology and altitude, this horizon may be roughly correlated to Layer 9 of the Laowogou section. The latter has yielded *Hipparion* sp., ?*Chilotherium* sp., *Axis shansius*, *Cervus* sp., *Antilospira* sp., etc. (as listed in Cai et al., 2004 and Cai et al., 2013). If taken as one unified fauna, they would represent a *Hipparion houfenense* fauna with considerable diversity.

On the one hand, the extensive existence of Pliocene strata on both sides of the Huliu River has been indicated by large mammal fossils from Luanshigedagou, Dannangou, and Huabaogou (Huang et al., 1974; Tang, 1980b; Wang, 1982) and small mammal fossils from Yuanzigou, Qijiazhuang, Jiangjungou, Laowogou, Hongyanangou, and Huabaogou (Zhang et al., 2003; Cai et al., 2004, 2013; Li et al., 2008). On the other hand, we have also noted that the magnetostratigraphic dating results published in recent years have placed the fossil bearing layer of Luanshigedagou, Hongya Village in between the "Gauss-Matuyama" boundary and the lower boundary of "Olduvai" (2.58–1.95 Ma); the upper fossil layer of Huabaogou, HBG-I, right above the upper boundary of "Olduvai" (<1.77 Ma); the lower fossil layer of Huabaogou, HBG-II, within "Olduvai" (1.95–1.77 Ma); the fossil layers of DD-1~7 of Daodi or Laowogou between the "Gauss-Matuyama" boundary and the upper boundary of "Olduvai" (2.58–1.77 Ma) (Zhu et al., 2007; Deng et al., 2008; Deng, 2011; Ao et al., 2013). Consequently, apparent contradiction occurs between these results and biostratigraphic correlations based on mammalian fossils. The features of the Yegou *Hipparion houfenense* fauna that is made up of only large mammals are also indicative of Pliocene age. Its establishment will accordingly provide additional evidence for the existence of the Pliocene in the Nihewan Basin and for the necessity of cautious reinterpretations of these magnetostratigraphic dating results.

Abbreviations F:AM, the Frick Collection of American Museum of Natural History; IVPP V/V, catalogue number of vertebrates of Institute of Vertebrate Paleontology and Paleoanthropology, Chinese Academy of Sciences (IVPP, CAS); IVPP RV/RV, revised catalogue number of vertebrates of IVPP, CAS; JNTZ, catalogue number of Nanjing Museum; NNNM, catalogue number of Nihewan National Nature Reserve; NWUV, catalogue number

of vertebrates of Northwest Universituy; THP, catalogue number of Tianjin Natural History Museum; ZKD, Zhoukoudian; L, length; W, width; Tri, trigonid; Min, minimum; Max, maximum.

2 Systematic descriptions

Nyctereutes tingi Tedford & Qiu, 1991

(Fig. 1)

Material Fragmentary right ramus with all teeth but the i2 and m3 (IVPP V 18833.1, Fig.1A); anterior portion of the fragmentary left ramus with c–p2 (V 18833.2); right m1 (V 18833.3, Fig.1B); right p4 (V 18833.4); fragment of the right ramus with the trigonid of the m1 (V 18833.5).

Measurements See Table 1.

Description The portion posterior to the m2 is not preserved on IVPP V 18833.1, so the development of the subangular lobe is unclear. The horizontal ramus, especially the anterior portion, is relatively robust. The ventral profile of the horizontal ramus is almost straight, but the ramus gradually deepens posteriorly. The depth is about 16.0 mm anterior to p3, and about 17.5 mm anterior to the m1. The symphysis is oval-shaped in lingual view, and its posterior margin slightly exceeds the posterior end of the p2 (Fig. 1A2). There are two mental foramina, with the anterior one being bigger and located below the diastema between the p1 and p2, and the posterior one being smaller and right below the p3 (Fig. 1A3).

The lower incisors are, well preserved with the exception of the i2, set obliquely on the ramus with the tip protruding dorsoanteriorly. The i1 is spatula-like with a truncated top and no cuspid lingually. The i2 is lost, leaving an oblong alveolus that is larger than that of the i1. The i3 is basically a triangular pyramid and distingctly larger than the i1 that is characterized by a

Table 1 Measurements of lower teeth of selected species in *Nyctereutes* (mm)

		N. tingi			*N. sinensis*			*N. procyonoides*
		Yegou		Yushe	ZKD Loc.1	Ningyang	Yushe	Yangyuan
		V 18833.1	V 18833.2–4	Tedford & Qiu, 1991	Pei, 1934	Zhang, 2001 V 12368.1–5, 8	THP10080 THP25646	V 2737
c	L	8.1	7.7	8.0–9.6	6.7	6.4	6.2	4.0
	W	5.1	5.4	5.3–6.0	5.2	4.2	4.0	3.4
p1	L	4.6	4.5	3.8–5.2	3.4–3.6	3.4–3.9	3.0–3.5	3.1
	W	3.0	2.9	2.8–3.8	2.1–2.7	2.2–2.3	2.1–2.3	1.3
p2	L	8.1	7.9	8.0–9.4	6.1–7.1	6.8–7.0	5.6–6.8	5.7
	W	3.4	3.7	3.6–4.1	2.8–3.2	3.0–3.1	2.9–3.2	2.2
p3	L	9.9		9.0–10.6	7.1–8.0	7.7–8.2	6.7–7.6	
	W	3.8		3.8–4.3	3.0–3.8	3.3–3.6	3.2–3.3	
p4	L	9.9	10.6	10.2–12.1	8.3–10.0	8.8–9.4	8.4–8.8	7.3
	W	4.6	4.3	4.9–5.9	4.0–5.0	4.3–4.4	3.4–4.2	3.3
m1	L	16.8	17.6	17.5–19.3	14.2–16.5	14.8–15.2	13.1–14.5	12.8
	W	6.9	7.2	6.7–7.9	6.3–7.2	6.0–6.5	5.7–6.2	5.1
m2	L	9.7		8.8–10.0	7.4–8.3	8.3	8.5	6.2
	W	6.8		6.0–7.5	4.4–5.8	5.2	6.0	4.8

feeble cuspid developed distally. The lower canine is conical and buccolingually compressed. The p1 is unicuspid and single-rooted. The p2, p3, and p4 are basically similar in both size and morphology. They are buccolingually compressed to some extent and possess a developed principal cusp. No accessory cusps are developed on either the p2 or p3, but there is a remarkable posterior accessory cusp on the p4. The protoconid is the dominant cusp on the m1, whereas the paraconid is slightly smaller and the metaconid the smallest. The talonid of the m1 is simple and bears only the hypoconid and entoconid. The former is higher than the latter. A transverse cristid between them divides the talonid into two parts, with the anterior part bigger than the posterior part (see Fig. 1B1). No accessory cusps or tubercles could be discerned on the talonid of the m1. The m2 is oval-shaped in occlusal view. The anterior half is broader than the posterior half. The metaconid is slightly taller than the protoconid, but they are similar in size. The talonid of the m2 bears a distinct hypoconid and a weak crest-like entoconid. No accessory cuspids are developed. A cingulid is slightly developed anterobuccally on the tooth.

IVPP V 18833.2 is a fragmentary left ramus. Only the portion anterior to the p3 is preserved. Its teeth, such as the c, p1, and p2, are generally similar to that of V 18833.1 in both size and shape. V 18833.3 is basically similar to the m1 of V 18833.1 in morphology, but slightly different in the development of a feeble tubercle on the posterior margin of the tooth (Fig. 1B1), which could be considered as the embryonic hypoconulid. V 18833.4 is a right p4, and similar to that of V 18833.1 in both shape and size. V 18833.5 bears a broken right m1. The preserved protoconid and metaconid are the same as that of V 18833.1 and V 18833.4 in morphology and no smaller than the latter two in size.

Fig. 1 Selected specimens of *Nyctereutes tingi* from Yegou
A. fragmentary right ramus with i1, i3, c and p1–m2 (IVPP V 18833.1, 2 cm scale bar);
B. right m1 (V 18833.3, 1 cm scale bar); 1. occlusal view, 2. lingual view, 3. buccal view

Comparisons and discussion Based on the morphology and size of the mandible and the lower carnassial (m1) summarized in Tedford et al. (1995, 2009) and Daguenet and Sen (2019), the Yegou specimens are undoubtedly assigned to *Nyctereutes* of Canidae.

The Yegou specimens are obviously larger than *Nyctereutes sinensis* from Yushe of Shanxi and Zhoukoudian, and extant *N. procyonoides* as well, but closer in size to *N. tingi* from Yushe (Table 1).

The ramus of V 18833.1 is relatively robust with the anterior half especially deep, and therefore different from *Nyctereutes sinensis*, which has anteriorly shallow but posteriorly deep ramus so that the dorsal margin of the ramus strongly slopes down anteriorly (see Tedford and Qiu, 1991:fig. 1B; Pei, 1934:fig. 5D). Consequently, the anterior portion of the ramus of *N. sinensis* is much slimmer, e.g., the depth of V 350-2 from Loc. 1 of Zhoukoudian is only 13.8 mm anterior to the p3, that of V 12368.1–2 from Ningyang of Shandong is only 11.2–13.3 mm. In terms of this feature, the Yegou specimen V 18833.1 is closer to the holotype of *N. tingi* F:AM 97030 from Yushe, the same dimension of which is 15.1 mm.

In addition, the m1 talonid of V 18833.1 and V 18833.3 is relatively simple in construction, bears no other tubercles except the hypoconid and entoconid, and consequently differs from *Nyctereutes sinensis*, since the m1 talonid of the latter somewhat tends to be complicated, e.g., the entoconid of *N. sinensis* from Loc. 1 of Zhoukoudian normally splits into 2–3 cuspids (Pei, 1934), and an extra cuspid, i.e., the hypoconulid, is even developed on the m1 of *N. sinensis* from Renzidong, Fanchang of Anhui (Liu and Qiu, 2009). It should be noted here that a transverse cristid developed between the hypoconid and entoconid, and subsequent division of the talonid into two unequal parts are the primary morphological features distinguishing *N. tingi* from *N. sinensis* (Tedford and Qiu, 1991). According to such morphological criterion, the Yegou specimens could be referred to *N. tingi* without any doubt, which further confirms the assertion of the existence of *N. tingi* in the Nihewan Basin proposed by Farjand et al. (2021).

The m2 is quite simple on V 18833.1 in morphology. Namely a cingulid is slightly developed only on its anterobuccal margin, and the entoconid is crest-like on the talonid with no other accessory cuspids except the entoconid and hypoconid. The Yegou specimens are exactly in accordance with *Nyctereutes tingi* in the morphology of m2 as well.

Based on the morphology and size of both the rami and teeth described above, the Yegou specimens are apparently closer to *Nyctereutes tingi* as a whole, although they are fragmentary and lacking certain key diagnostic parts, such as the subangular lobe and angular process of the mandible, etc.

Nyctereutes tingi was originally established based on the material from the Mazegou and Gaozhuang formations in the Yushe Basin (Tedford and Qiu, 1991). It is a fairly primitive species at an evolutionary stage that can be roughly correlated to *N. donnezani* of Ruscinian from Europe. The species was also reported at Lingtai of Gansu (Huang et al., 1993) and Danangou of the Nihewan Basin (Farjand et al., 2021). The known records indicate that *N.*

tingi is distributed only in Pliocene strata. For that reason, the discovery of *N. tingi* at Yegou proves that the Pliocene strata does exist in the Nihewan Basin.

Fossil *Nyctereutes* has a continuous stratigraphic distribution in the strata from Early Pliocene onwards in China and has an evolutionary trend of gradual reduction in body size (Pei, 1934; Teilhard de Chardin and Pei, 1941). The dental measurements of *N. tingi* from the Yushe Basin clearly reveal such a trend: teeth from the Gaozhuang Formation are generally larger than those from the Mazegou Formation (based on WANG Xiao-Ming's unpublished data). In dental size, the material from Yegou is much closer to that from the Mazegou Formation (Late Pliocene), but smaller than that from the Gaozhuang Formation (Early Pliocene).

***Nyctereutes sinensis* (Schlosser, 1903)**

(Fig. 2)

Material Fragmentary cranium lacking the rostrum (IVPP V 18834.1, Fig. 2), fragmentary right ramus with the m2 (V 18834.2), fragmentary right ramus with only alveoli of the p1–3 preserved (V 18834.3)

Measurements See Table 2.

Description V 18834.1 is an incomplete cranium. The nasals, premaxillae and maxillae are broken off, and both of the zygomatic arches and the right tympanic bulla are also missing. It is distinctly larger than the extant species *Nyctereutes procyonoides*. In lateral view, the dorsal profile of the frontal and parietal first runs posterodorsally and reaches its highest point approximately above the postglenoid process, then it runs horizontally posteriorly (Fig. 2D, E). In dorsal view, the frontal area is fairly broad, and its maximal breadth between the postorbital processes is 53.5 mm, which is comparable to the greatest neurocranium breadth. The central portion of both frontals bulges strongly. Consequently, a deep depression is formed along the frontal suture between the frontals. The vulpine groove is also developed on the surface adjacent to the frontal postorbital process, which indicates that the frontal sinus is developed but does not expand into the tip of the postorbital process. The postorbital process is rather robust. The posterodorsal rim of the orbit is not straight but curved and concave. The strong and ridge-like parasagittal crest also makes a concave curve and extends from the postorbital process posteromedially and joins its counterpart slightly posterior to the frontoparietal suture, which makes the postorbital process very pointed (Fig. 2A). The sagittal crest is also massive and sticks out of the parietal surface about 3.0 mm. The sagittal crest, especially its anterior portion, is broad, and a central longitudinal groove runs throughout along the midline. The postorbital constriction is not strong, and the width is 37.1 mm, which is broader than the distance between the orbits (less than 33.2 mm) and about the same as the braincase width. The surface of the parietal is relatively smooth, and not as rough as that of the extant species. In ventral view, the tympanic bulla is strongly inflated, especially at the middle and posterior portions. The anterolateral side is less dilated, and the anterior margin aligns with the postglenoid process and does not exceed it (Fig. 2B).

V 18834.2 is a fragmentary ramus with only the m2 still in position. The dorsal profile

of the horizontal ramus significantly slopes down anteriorly. As a result, the anterior portion of the ramus is shallower, with a depth of only 14.4 mm anterior to the p3. The m2 (about 5.9 mm in width) is similar to that of V 18833.1 of *Nyctereutes tingi* in morphology, but evidently narrower. A cingulid is developed anterobuccally, and more distinct than in V 18833.1. The metaconid is quite small but discernible.

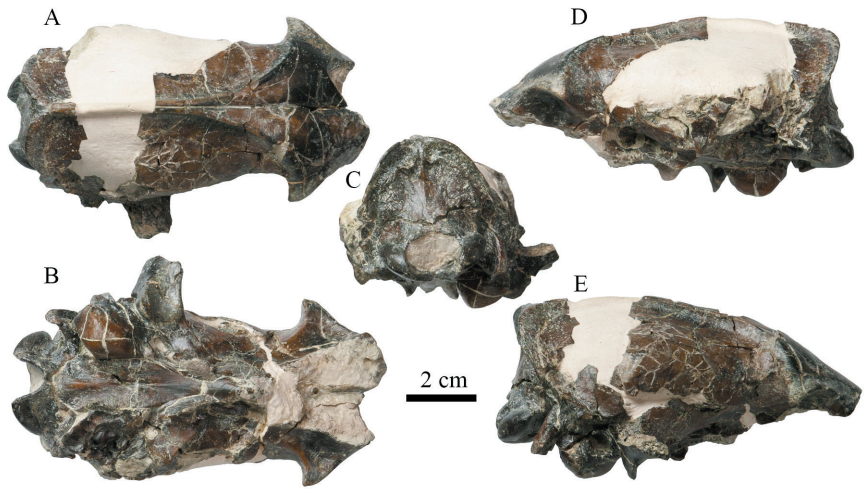

Fig. 2 Fragmentary cranium of *Nyctereutes sinensis* (IVPP V 18834.1) from Yegou
A. dorsal view, B. ventral view, C. occipital view, D. left lateral view, E. right lateral view

V 18834.3 only has preserved the portion anterior to the p4, including the alveoli of p1–3. The anterior portion of the ramus is shallower, and the depth is about 13.2 mm anterior to the p3.

Comparisons and discussion Although the cranium of V 18834.1 is incomplete, the preserved portion could be compared with the species in *Nyctereutes*. It is distinctly larger than the extant *N. procyonoides*, but roughly comparable in size to *N. sinensis* from Yushe of Shanxi (Table 2).

Regarding the cranium morphology, V 18834.1 appears to have combined characteristics of both *Nyctereutes sinensis* and *N. tingi*. On the one hand, V 18834.1 is quite similar to the specimen JNTZ 7571 of *N. sinensis* from Tuozidong, Nanjing in the following aspects: 1) almost equal size; 2) robust, pointed and protruding postorbital process; 3) curved and ridge-like parasagittal crest; 4) high and broad sagittal crest with a central longitudinal groove running throughout; and 5) anterior margin of the tympanic bulla not exceeding the postglenoid process (Liu et al., 2007:26, fig. 2.4). Moreover, the cranium V 18834.1 also resembles that of *N. sinensis* (=Liu, 2019: *Nyctereutes* cf. *N. tingi*) from the Nihewan Basin described by Liu (2019), such as NNNM 13–18 (see Liu, 2019: fig. 23), in all the features listed above except for the 5th one. Nevertheless, it is worth noting herein that neither central bulging of the frontal nor the depression along the frontal suture could be discerned in JNTZ 7571 and NNNM 13–18.

On the other hand, V 18834.1 is also similar to the specimens of *Nyctereutes tingi* from Yushe of Shanxi in the following characteristics: 1) the dorsal profile of the parietal is relatively flat but not convex in lateral view; 2) the neurocranium is laterally inflated so poorly that its maximal width is almost equal to that across the postorbital processes; and 3) the postorbital constriction is so weak that its width is evidently greater than the distance between the orbits.

Table 2 Measurements of the crania of selected species in *Nyctereutes* (mm)

	N. sinensis				*N. procyonoides*[2)]		
	Yegou	Yushe	ZKD Loc.13[1)]		Min	Max	Mean
	V 18834.1		Skull A	Skull B			
basioccipital length		147.0	135.0	~120.0	104.0	117.0	110.0
zygomatic width		85.0	~84.0	~63.0	57.0	68.5	61.9
width between mastoid processes	~53.9	52.0	49.0	~44.0	38.0	43.0	40.4
postorbital constriction width	37.1	36.0	23.0	21.0			
distance between orbits	33.2	32.0	30.0	25.0			
greatest neurocranium width	~50.1	53.0	51.0	45.0	32.0	43.0	39.6
maximal palatal width		45.0	43.0	38.0	33.0	37.0	34.9

1) from Teilhard de Chardin and Pei (1941); 2) from Allen (1938)

As a whole, nevertheless, the Yegou specimens seem closer to *Nycetreutes sinensis*, with reservation of some primitive features similar to *N. tingi*. It should be noted herein that the cranium V 18834.1 is incomplete, and the analysis mentioned above is largely based on the reconstruction (see the white plaster part in Fig. 2). Whether the reconstruction is constructed correctly has a direct bearing on the conclusion of the similarity between V 18834.1 and *N. tingi*. In other words, its similarity to *N. tingi* can not be assured at the moment. Under such circumstances, it seems more reasonable to assign the Yegou specimens described herein to *N. sinensis*. And if that's the case, there would be occurrence of both *Nyctereutes* species at Yegou, Nihewan Basin, a similar case like in the Yushe Basin (Tedford and Qiu, 1991).

The morphological differences between V 18834.2–3 and V 18833.1 are as follows: 1) the ramus of the former is relatively slim, the anterior portion of which is especially shallow and the dorsal profile of which slopes signifcantly; 2) the m2 is relatively narrow, but the cingulid and entoconid are much better developed on the tooth. In these morphological characters, nevertheless, V 18834.2–3 exactly show the diagnostic features for *N. sinensis*.

In terms of the chronological distribution, *Nyctereutes sinensis* has extensive Late Pliocene and Early Pleistocene records, such as those from the Yushe Basin of Shanxi (Tedford and Qiu, 1991), the Nihewan Basin of Hebei (Teilhard de Chardin and Piveteau, 1930; Liu, 2019), Wushan of Chongqing (Huang and Zhong, 1991), Ningyang of Shandong (Zhang, 2001), Fanchang of Anhui (Liu and Qiu, 2009), Mianchi of Henan (Zdansky, 1924), Tuozidong, Nanjing of Jiangsu (Liu et al., 2007), and so on. In addition, some *Nyctereutes* fossils from Middle Pleistocene horizons, such as Loc. 13 and Loc. 1 of Zhoukoudian, were also assigned to *N.* "*sinensis*" (Pei, 1934; Teilhard de Chardin and Pei, 1941), but the systemtic identification of these *Nyctereutes* fossils is still doubtful and disputed. In terms of

morphology, they are actually closer to the extant species rather than the earlier fossil species (Soria and Aguirre, 1976; Tedford and Qiu, 1991).

The differences between the Yegou specimen V 18834.1 and the Zhoukoudian specimens of *N.* "*sinensis*" lie in the following features: the frontal postorbital process of the former is more protruding; the postorbital constriction is not strong; the surface of the parietal is relatively smooth. All these features are basically consistent with the *Nyctereutes* fossils from Nihewan and Tuozidong, Nanjing (Teilhard de Chardin and Piveteau, 1930; Liu et al., 2007; Liu, 2019). The morphology of V 18834.1 actually presents one more support for the judgement and analysis of Soia and Aguirre (1976), Tedford and Qiu (1991), and so on.

If the reconstruction of V 18834.1 is reliable, it would be slightly more primitive than the other known crania assigned to *Nyctereutes sinensis* (such as those from Nihewan and Tuozidong) with a flat parietal and less dilated neurocranium. In this respect, the specimens described herein seem to be no later than that from the Mazegou Formation of the Yushe Basin in age.

***Pachycrocuta pyrenaica* (Depéret, 1890)**

(Fig. 3)

Material Fragmentary ramus with p3–m1 (IVPP V 18835, Fig. 3).

Measurements See Table 3.

Description V 18835 is a left broken ramus with an absence of the portion anterior to the p3 and most of the ascending ramus. The horizontal ramus is relatively slim. The depth is 37.7 mm anterior to the p3, and 43.4 mm posterior to the m1, respectively. In occlusal view, the p3, p4 and m1 are almost rectangular in shape. The principal cusp of the p3 leans posteriorly and is massive but compressed buccolingually. The posterior accessory cusp is low. There is no discernible anterior accessory cusp developed, but a swollen enamel ridge is formed anteriolingually around the base of crown, probably representing a rudimentary cuspid. Feeble cingulids are discernible at the anterior and posterior margins of the tooth. The p4 is slightly larger than the p3. The principal cusp is robust and tall but leans posteriorly. It has anterior and posterior accessory cusps of equal size. The three cusps align almost in a straight line oblique to the long axis of the tooth, with the anterior accessory cusp positioned lingually and the posterior one buccally. The anterior cingulid is less developed than the posterior one. The anterior portion (where the paraconid is located) of the m1 is slightly broader than the posterior portion (the talonid). The paraconid is slightly longer than the protoconid, but they are almost equal in height. The metaconid is developed at the posterolingual corner of the protoconid, with only half the height of the latter. The two cusps are separated by a shallow groove. The talonid is robust and broad, and the trigonid is only 78% of the total length of the tooth. The hypoconid and entoconid are distinct. The hypoconid is almost displayed as a ridge parallel to the long axis of the tooth. The entoconid is low and conical on the lingual side. There is a curved ridge connecting the hypoconid and entoconid at the posterior margin of the talonid. Several cuspids or tubercles developed on it could be regarded as the rudimentary

hypoconulid. A weak cingulid is developed on both the anterior and posterior margins of the tooth, respectively.

Comparisons and discussion In terms of dental size and morphology, the Yegou specimen described above (especially the m1) is conspicuously closest to *Pachycrocuta* in the Hyaenidae. It could be distinguished from *P. brevirostris* and *P. licenti* by its smaller size, relatively narrow premolars and an m1 with the more developed metaconid and talonid. The Yegou specimen virtually approximates *P. pyrenaica* and *P. perrieri* in both size and morphology.

In dental length, the Yegou specimen is nearly the same as *Pachycrocuta pyrenaica* and *P. perrieri*, and completely falls in the variation range of these two species (Table 3), but in dental width, the Yegou specimen is closer to *P. pyrenaica* from Yushe of Shanxi, and distinctly narrower than *P. perrieri* (distinctly less than the mean of it, see Table 3). Morphologically, *P. pyrenaica* is different from *P. perrieri* in its much narrower premolars (mainly P2/p2, P3/p3) (Howell and Petter, 1980; Qiu, 1987).

It seems not convincing enough to identify a species solely on the basis of tooth size. The lower carnassial of V 18835 would provide extra robust evidence for that. *Pachycrocuta pyrenaica* is relatively primitive in shape: the shearing blades of the carnassials (the P4 and m1) are relatively short. It is shown as a lower value in the proportion of the trigonid to the total length of the tooth on the m1 (i.e., Tri/m1 in Table 3) (Howell and Petter, 1980). The trigonid of the Yegou specimen is relatively short (about 78% of the total length) and comparable to *P. pyrenaica* from other localities, but shorter than *P. perrieri* (completely out of

Table 3 Measurements of the lower teeth of selected species in *Pachycrocuta* (mm)

		P. pyrenaica					*P. perrieri*
		China		Ukraine	France	Tunis	France
		Yegou	Yushe	Odess Catacomb	Serra d'en Vacquer	Ain Brimba	Etouaires[1)]
		V 18835	Qiu, 1987	Howell and Petter, 1980			
		range,mean(number)					
p3	L	21.2	21.2–20.1, 20.68(5)	21.8–14.0, 20.02(19)	20.0	21.5	22.9–19.5, 20.93(16)
	W	13.2	13.3–13.0, 13.24(5)	14.2–11.9, 12.89(19)	13.3	13.7	16.6–13.3, 14.52(13)
	W/L	0.62	0.66–0.61, 0.64(5)	0.68–0.61, 0.64(19)	0.67	0.64	0.78–0.63, 0.69(13)
p4	L	22.5	22.5–21.5, 22.05(6)	24.0–20.5, 22.25(22)	24.4	23.4	25.5–21.4, 23.46(19)
	W	12.6	13.3–13.1, 13.25(6)	14.3–12.2, 12.75(21)	13.3	13.3	16.1–11.8, 14.62(16)
	W/L	0.56	0.61–0.59, 0.60(6)	0.60–0.52, 0.57(21)	0.55	0.57	0.64–0.60, 0.62(16)
m1	L	25.0	27.1–23.2, 25.35(4)	28.7–23.1, 24.82(21)	24.7	24.5, 24.5	26.9–23.4, 25.44(22)
	W	12.0	12.4–11.6, 12.05(4)	12.2–10.4, 11.42(21)	12.6	11.1, 11.3	14.6–10.8, 12.80(16)
	Tri L	19.4	21.6–18.8, 20.16(5)	20.7–17.4, 18.77(20)	19.2	19.9, 19.4	22.8–19.4, 21.41(19)
	Tri/m1	0.78	0.81–0.78 0.80(4)	0.81–0.72, 0.76(21)	0.78	0.81, 0.79	0.86–0.81, 0.83(19)

1) including Etouaires, St-Vailler, Seneze of France, Val d'Arno of Italy, and Villarroya, Puebla Valverd of Spain.

the variation range of the latter, see Table 3). Moreover, the metaconid of the m1 usually is reduced or vanishes in *P. perrieri* (Howell and Petter, 1980; Qiu, 1987). For example, the metaconid on the m1 of JNTZ 6401 from Tuozidong, Nanjing is vestigial in the shape of an enamel tubercle on the posterolateral side of the protoconid near its base (Liu et al., 2007). The metaconid on the m1 of the Yegou specimen is small, but it is completely separated from the protoconid by a distinct shallow notch and acting as an independent cusp (see Fig. 3B, C), which is quite differtent from the vestigial metaconid on the m1 of *P. perrieri*.

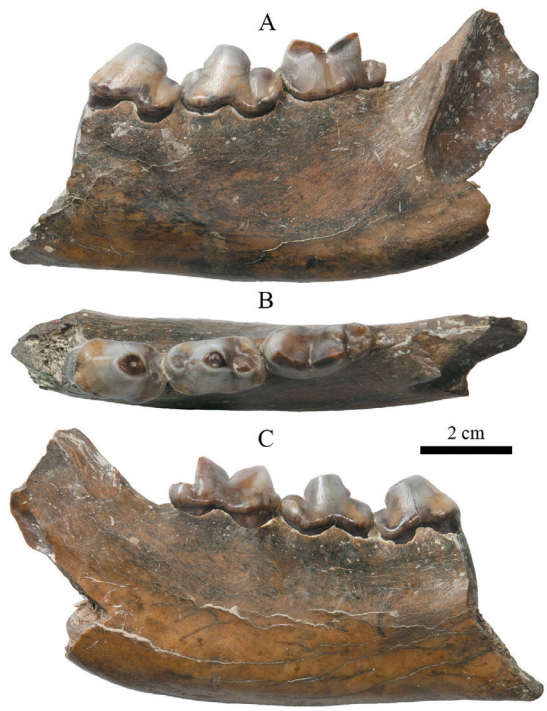

Fig. 3 Fragmentary right ramus of *Pachycrocuta pyrenaica* with p3–m1 (IVPP V 18835) from Yegou
A. buccal view, B. occlusal view, C. lingual view

Pachycrocuta pyrenaica was first discovered at Serrat d'en Vacquer, France. Depéret (1890) originally named it as *Hyaena arvernensis* var. *pyrenaica*. However, "*Hyaena arverensis*" should be a junior synonym of "*Hyaena perrieri*" (Howell and Petter, 1980; Qiu, 1987). In fact, as early as in 1954, Viret already clarified the situation, but emphasized that the specimens from Serrat d'en Vacquer, France, didn't belong to perrieri at all, but represented another independent species "*Hyaena donnezani*" (Viret, 1954). Howell and Petter (1980) attributed the authorship of the species name to Charles Depéret based on the principle of priority. They also pointed out that the species didn't belong to the extant genus Hyaena Brisson, 1762, but to the fossil genus *Pachycrocuta* Kretzoi, 1938. The name of the species was consequently revised as *P. pyrenaica* (Depéret, 1890).

Regarding size and morphology, certain similarities do exist between *Pachycrocuta pyrenaica* and *P. perrieri*. Sometimes it is difficult to distinguish them from each other. As a result, *P. pyrenaica* was even questioned to be a probable synonym of *P. perrieri* (Werdelin and Solounias, 1991; Turner et al., 2008). The Yegou specimen V 18835 bears the typical morphology of *P. pyrenaica* (based on the standard of Howell and Petter, 1980), which provides powerful surport for the validity of the species. If only the dental length is taken into consideration, it would be difficult more or less to differentiate the Yegou specimen from small-sized *P. perrieri*. For example, taking the Yegou specimen V 18835 as *P. pyrenaica* and the Tuozidong specimen JNTZ 6401 from Nanjing as *P. perrieri*, the length of the p3, p4 and m1 would be 21.2, 22.5, 25.0 and 20.8, 23.0, 25.8 mm, respectively, while the corresponding width would be 13.2, 12.6, 12.0 and 14.5, 14.4, 13.6 mm, respectively. It is easy to notice that

the p4 and m1 of V 18835 are slightly shorter than that of JNTZ 6401, but on the contrary, its p3 is longer than that of the latter. Nevertheless, the teeth of V 18835 are distinctly narrower than those of JNTZ 6401 (data for the latter from Liu et al., 2007). In addition, JNTZ 6401 could also be distinguished from V 18835 in m1 in the following characteristics: the relatively long trigonid (21.6 mm, 83.7% of the total length); the short talonid; and the reduced metaconid as a dependent tubercle. The present authors have no intention of discussing in depth the validity of *P. pyrenaica*, which is beyond the scope of the present paper, but the Yegou specimen of V 18835 would provide a good example to support the conclusion of Viret (1954) and Howell and Petter (1980).

In terms of morphology, *Pachycrocuta pyrenaica* is undoubtedly more primitive than *P. perrieri*, which is probably derived from the former (Schütt, 1972; Howell and Petter, 1980; Qiu, 1987). Their geochronological distribution also supports the following hypothesis: *P. pyrenaica* was only found in the strata before Villafranchian in Europe, such as Serrat d'en Vacquer of France (Depéret, 1890), Layna (Crusafont and Sondaar, 1971) and La Calera II (Adrover et al., 1976) of Spain, and Odessa Catacomb of Ukraine (Howell and Petter, 1980), while *P. perrieri* occured slightly later in the strata of Villafranchian and afterwards, such as Etouaires (Croizet and Jobert, 1828) and Saint-Vailler (Viret, 1954) of France, Villaroya and Puebla de Valverde of Spain (Croizet and Jobert, 1828), ValdArno of Italy (Weithofer, 1889), Hajnáčka of Slovakia (Fejfar, 1964) and so on. Fossil records of *P. pyrenaica* are relatively scarce in China, only known from Yushe of Shanxi (Qiu, 1987) and Zanda of Xizang (Tseng et al., 2016, =*P. perrieri*). In contrast, records of *P. perrieri* are more extensive. It has been known from Yushe of Shanxi and the Nihewan Basin of Hebei (Qiu, 1987), Ningyang of Shandong (Zhang, 2001), Tuozidong, Nanjing of Jiangsu (Liu et al., 2007), Wushan of Chongqing (Huang and Zhong, 1991, =*P. licenti*; Zhang, 2001), and Shanyangzhai, Qinhuangdao of Hebei (Liu, unpublished). The geochronological distribution of the two *Pachycrocuta* species in China is similar to that in Europe. Except in the Yushe Basin, *P. perrieri* is only distributed in the Early Pleistocene (equivalent to middle and late Villafranchian). Although *P. perrieri* and *P. pyrenaica* co-occurred in the Yushe Basin, the former is only known from the upper part of the Mazegou Formation, the age of which is equivalent to the early Villafranchian, while *P. pyrenaica* is known from the lower part of the Mazegou Formation, the Gaozhuang Formation, and even the Mahui Formation, the age of which is equivalent to or even older than the Ruscinian (Qiu, 1987; Deng and Hou, 2011). The discovery of *P. pyrenaica* at Yegou, the Nihewan Basin not only expands the distribution of this species but also provides reliable evidence to determine the age of the Yegou fauna.

***Homotherium* sp.**

(Fig. 4)

Material Anterior half of left ramus with the i2, c, and p4 (IVPP V 18836.1, Fig. 4); fragmentary right ramus with i3 (V 18836.2).

Measurements See Table 4.

Description V 18836.1 is the anterior half of a left ramus with the portion posterior to the p4 missing. The symphysis is well preserved with the portion beneath the canine slightly broken. In rostral view, the symphysis is nearly rectangular with a height greater than the width. Multiple nutrient foramina could be discerned on the surface. In lingual view, the symphysis has a nearly vertical rough surface. The upper part is slightly wider than the lower. The posterior margin terminates approximately at the posterior edge of the canine (Fig. 4C). In buccal view, the mesial portion of the symphysis, especially the upper third, distinctly protrudes anteriorly so much that the incisor row is conspicuously anterior to the canine (Fig. 4A). The ventral margin of the symphysis is at about the same level as that of the horizontal ramus due to the missing mandibular flange, but the dorsal margin of the symphysis is apparently higher than that of the horizontal ramus, so the implant positions for the incisor and canine are higher than the cheek teeth (Fig. 4A, C). The robust ridge-like mental crest is developed beneath the canine, but most of the ventral portion is missing, and the mandibular flange is missing as well. However, judging from the surrounding structures, the mandibular flange might be very well developed. The p1 and p2 are not developed at all, so there is a diastema of 38.1 mm between the canine and p3. The dorsal margin of the ramus within the diastema slopes up anteriorly from the anterior end of the p3. Approximately beneath the midpoint of the diastema, a mental foramen of 10.7 mm in diameter is developed right above the ventral margin of the ramus. There is another mental foramen of 6.6 mm in diameter posterodorsal to the anterior mental foramen. The distance between them is 14.0 mm. Beneath the smaller mental foramen, there is an anteroventrally running ridge, which indicates the existence of a mandibular flange (although not preserved). In occlusal view, the dorsal edge of the diastema forms a sharp crest that is lingually concave (Fig. 4B).

In occlusal view, the incisors and the canine are densely aligned and form a unitary anteriorly convex arc (Fig. 4B). The i1 and i3 have already fallen off. Only the oval alveoli are preserved. Judging from the shape of the alveoli, i1 to i3 are gradually increasing in size. The i2 is conical and slightly bends posteriorly. There are two distinct crests developed on the anteromedial and posterodistal sides respectively. Both crests are serrated, but the posterodistal one is sharp. Although the p3 has shed off, the gourd-shaped alveolous (length/width: 12.9 mm/7.4 mm) clearly indicates that the tooth has two detached roots. The p4 is large and compressed buccolingually. In occlusal view, it appears approximately rectangular. The principal cusp is robust, tall and leans posteriorly. Two thin and sharp lateral crests run from the principal cusp forward and backward respectively. The anterior lateral crest is serrated. The two blunt-tipped accessory cusps are nearly equal in size and height. There is a second cuspid posterior to the posterior accessory cusp. A weak cingulid is developed only on the posterolingual margin of the tooth.

Comparisons and discussion Although the material is quite limited, a series of important anatomical features have been revealed: the mental crest and mandibular flange are developed at the symphysis; the incisor row is anteriorly convex; the canine, incisors and molars

have lateral crests with serration; the implant position of the incisors and canine is higher than that of the check teeth. By these convincing features, the Yegou specimens described above should be undoubtedly assigned to the sabre-tooth group, namely the Machairodontinae. Based on the size and the morphology of the mandibular flange and the mental crest, they should definitely be excluded from *Megantereon*. Consequently, only *Machairodus* and *Homotherium* are applicable herein for futher discussion about its assignment.

Table 4 Measurements of the lower teeth and mandibles of selected machairodontines (mm)

		Homotherium						*Machairodus*	
		Homotherium sp.				*H. crenatidens*		*M. kurteni*	*M. horriblis*
		Yegou	Yushe			Renzidong	Seneze	Kalmakpai	Baode
		V 18836.1	RV 45018 left	RV 45016	RV 45017 right	V 13675.1	Ballesio, 1963	Sotnikova, 1992	V 15643 right
symphysis depth		69.3	79.7	60.1	59.5	70.3	71.0	72.5	80.0
c–i1 width		30.3	27.8	29.3	27.5	29.4			35.6
corpus depth anterior to p3		45.9	46.8	34.7	35.8	44.1	45.0	39.0	44.3
corpus depth anterior to p4		41.7	44.9	~33.1	35.1	41.6			44.9
c–p3 diastema width		38.1	44.2	36.9	38.3	46.5	37.0	37.7	55.2
c	L	16.6	15.4	14.8	17.6	16.6		16.2	19.6
	W	11.1	10.9	10.6	11.2	10.4		11.6	13.2
p3	L	12.9*	11.2*	13.8*	11.1	6.5	8.0	17.5	19.2
	W	7.4	6.7	8.2	6.2	5.1	5.5		10.1
p4	L	24.8	17.0*	21.2	21.8	21.1	22.0	26.8	33.5
	W	11.4	8.9	10.0	9.2		11.0	11.5	14.0
c–p4 L		93.6	95.3	89.3	90.1	91.6+	>88.0	>97.0	131.7
corpus thickness at p4		18.9	18.4	15.8	15.5	19.3	18.0		20.9

* alveolus; + right.

It is generally accepted that *Machairodus* and *Homotherium* are phylogenetically close to each other with the latter probably derived from the former (de Beaumont, 1975, 1978; Kurtén and Anderson, 1980; Sharapov, 1989; Sotnikova, 1992; Liu, 2003). It is not troublesome to distinguish the two genera when the specimens are plentiful and complete. However, it is rather difficult when the material is scarce and fragmentary. Teilhard de Chardin and Leroy (1945) once assigned the 3 mandibles from Yushe (RV 45016–45018 in Table 4, Teilhard de Chardin and Leroy, 1945: fig. 6) to *Machairodus palanderi* (=*Epimachairodus palanderi*). Judging from the current knowledge, there seem to be at least two differences between these mandibles of Yushe and other mandibles identified as *Machairodus*: 1) the Yushe specimens are smaller, especially RV 45016 and RV 45017 (see measurements in row 1, 3, 4, 9, 10 of Table 4), and even smaller than *M. kurteni*; 2) the premolars of both the large individual (RV 45018) and the slender individuals (RV 45016 and RV 45017) are smaller than the species of *Machairodus*, especially the p3. In *Machairodus*, the p3 is generally large. Even in *M. palateri* that has a relatively reduced p3, its length can still reach 15.1 mm (Zdansky, 1924); the p3 usually has bifurcated two roots (Sharapov, 1989; Sotnikova, 1992:fig. 4); there are 2–3 cusps developed on the p3 (Sotnikova, 1992; Anton et al., 2004; Qiu et al., 2008). Among the

mandibles from Yushe, the p3s of RV 45016 and RV 45018 are single-rooted; the p3 of RV 45017 is likely to be two-rooted, but they are fused together at least at the upper part; the p3s of RV 45016 and RV 45018 have fallen off, and only the alveolous is preserved; the p3 of RV 45017 is preserved, but it has only one cusp. It can thus be concluded that compared with the Miocene species of *Machairodus*, the p3 of the Yushe specimen has been greatly reduced, so the assignment of them to *Machairodus* is not convincing.

Sotnikova (1992) pointed out the differences between *Machairodus* and *Homotherium* in the implant and arrangement of their incisors and canine when studying the specimens of

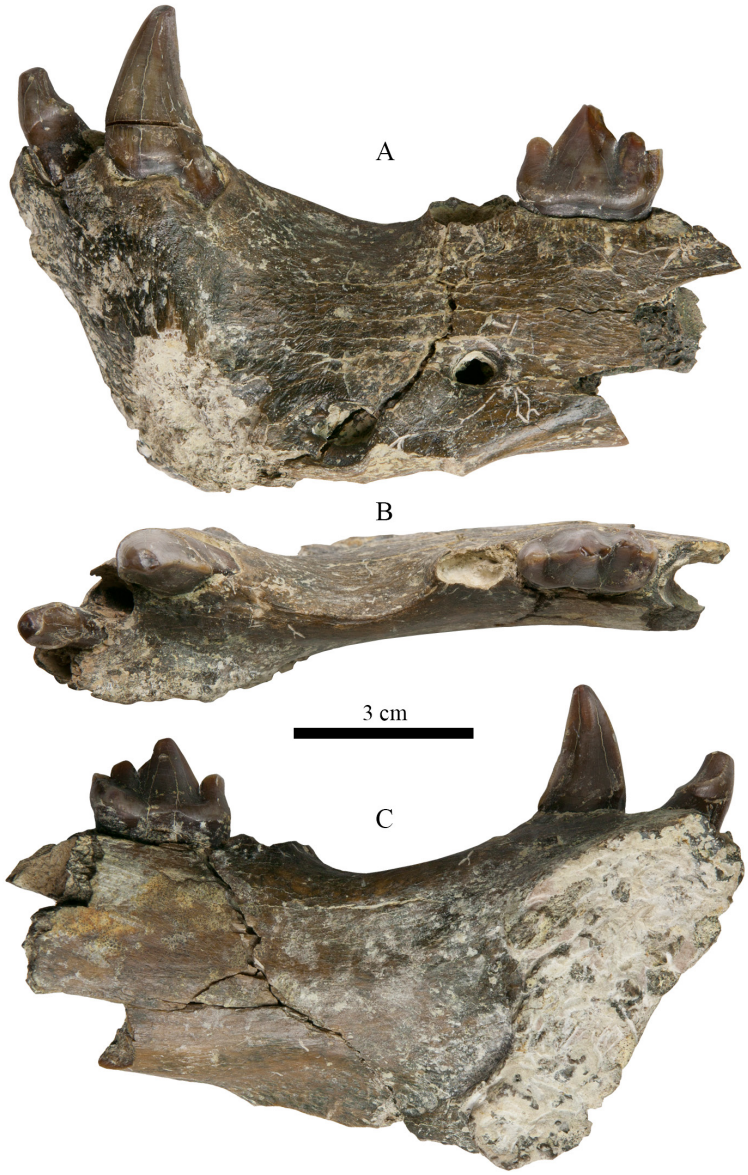

Fig. 4 Fragmentary left mandible of *Homotherium* sp. with i2, c and p4 (IVPP V 18836.1) from Yegou
A. buccal view, B. occlusal view, C. lingual view

M. kurteni from Kazakhstan. In *Homotherium*, the incisors and canine are densely aligned, so there is no gap between the central incisor and the canine; the incisors are upright and their tips are dorsally pointing. In *Machairodus*, there is a small gap between the canine and the incisors; the incisors are implanted obliquely with the tips pointing anterodorsally. Judging from these differences, the Yushe specimens are apparently consistent with *Homotherium*, but distinct from *Machairodus* (see Teilhard de Chardin and Leroy, 1945:fig. 6).

Nonetheless, the Yushe specimens are not completely the same as *Homotherium*. RV 45018 is relatively robust. Its mandible is comparable to that of *Homotherium crenatidens* from Renzidong, Anhui and Seneze, France, while RV 45016 and RV 45017 are distinctly slenderer. Moreover, their p3 is relatively developed and markedly larger than those later species in *Homotherium* (see Table 4). How to identify the Yushe specimens is obviously beyond the scope of this paper, but at least two conclusions could be drawn herein from above comparisons: 1) they should be assigned to *Homotherium* rather than *Machairodus*; 2) they probably represent a relatively primitive form in the *Homotherium* clade, which is consistent with the age of the stratum they came from.

Although the assignment of the Yushe specimens to *Homotherium* is not confirmed at the moment, the Yegou specimen shows some unambivalent morphological features of *Homotherium*. The incisors and the canine are densely aligned with no gap between them. The incisors are upright and pointing dorsally. The incisors and the canine are so aligned that they form an anteriorly convex arc with the mesial ones more anteriorly implanted. There are serrations on all the preserved teeth. The last two features are more developed than the species of *Machairodus*. Moreover, the size and robustness of the mandible are completely consistent with that of *H. crenatidens* from Renzidong, Anhui (see Table 4). The only difference is its bigger premolars.

Presently, the taxonomical significance of the size of premolars (mainly the P3 and p3) among *Homotherium* species is still disputed. As a highly specialized felid, the anterior premolars of *Homotherium* probably have lost their physiological function. Under such circumstances, the size and morphology of those nonfuctional premolars would change significantly. For that reason, it is highly dangerous to distinguish species based on these changes (e.g., Ficcarelli, 1979).

However, judging from the general evolutionary trend of *Homotherium*, the gradual degeneration of the premolars is an indisputable fact. Their morphology (e.g., cusp and root) and size virtually reflect the evolutionary stage of the species. *Homotherium* might consequently be divided into several different evolutionary stages or different species (e.g., Sharapov, 1989). To that end, the authors observed and measured some specimens (see Table 4) and found that the evolutionary stages of *Homotherium* could indeed be established roughly. For the species of the middle Villafranchian and afterwards (e.g., Renzidong, Anhui and Seneze, France), the length of the p3 generally does not exceed 10.0 mm. The p3 of *H. cuii* from Middle Pleistocene Jinniushan is completely lost (Zhang et al., 1993). For the species

of and before the early Villafranchian (e.g., Yushe, Shanxi), the length of the p3 is generally no less than 10.0 mm. The length of the p3 alveolous of the Yegou specimen is 12.9 mm and comparable to RV 45016 from Yushe. It is much larger than the species of the middle Villafranchian and afterwards. Based on the measurements in Table 4, the Yegou specimen is situated somewhere in between *Machairodus* kurteni from Kazakhstan and *H. crenatidens* from Renzidong of Anhui, and most likely is a transitional form between them (relatively speaking, the Yushe specimens are not good enough to represent such transitional form: the teeth of RV 45018 are somewhat distorted while the mandibles of RV 45016 and RV 45017 are so slender that they probably represent a different phylogenetic clade). It could be inferred herein that the Yegou specimens probably represent an early form of *Homotherium* or an earliest representative of *H. crenatidens* (because the morphology and size of the mandible V 18836.1 are highly consistent with the specimens from Renzidong of Anhui). Unfortunately, V 18836.1 is the only identifiable specimen collected at Yegou. It is impossible to evaluate and analyse the variation of the p3 comprehensively, and the possibility of the big-sized p3 of V 18836.1 as an individual variation can not be ruled out at the moment. Although the premolars of *Homotherium* generally tend to be reduced, some individuals with extreme variation did occur time and again. For example, *H. crenatidens* from Val d'Arno of Italy have reduced premolars, but there is still one p3 with a length of 12.0 mm (Ficcarelli, 1979), comparable to the Yegou specimen. If only based on such an isolated p3, it would be less credible to presume that the Yegou specimen as an early primitive form of *Homotherium*. Nonetheless, if the associated animals, such as *Nyctereutes tingi* and *Pachycrocuta pyrenaica*, are taken into account, the present authors would be more confident of such a presumption, and consequently identify the Yegou specimens herein as *Homotherium* sp. for the moment. Further identification and inference still await more and better material in the future to be clarified.

Hipparion (*Plesiohipparion*) *houfenense* Teilhard de Chardin & Young, 1931

(Figs. 5–6)

Material Fragmentary right maxilla with the P3–M2 (IVPP V 18837.1, Fig. 5C) and left and right mandibular corpora with the p2–m3 (V 18837.2, V 18837.3, Fig. 5A) of the same individual, fragmentary right maxilla with the M1–3 (V 18837.4), 1 left and 1 right P2 (V 18837.5–6), fragmentary right mandibular corpus with the p2–m3 (V 18837.7, Fig. 5B), distal portions of two right humeri (V 18837.8, Fig. 6D; V 18837.9), proximal portion and distal portion of the same left Mc III (V 18837.10, Fig. 6A; V 18837.11), proximal portion of the left Mc IV (V 18837.12), right talus (V 18837.13, Fig. 6E), right calcaneus (V 18837.14, Fig. 6G), proximal portion of the right Mt III (V 18837.15, Fig. 6B), proximal portion of the right Mt II (V 18837.16, Fig. 6C), and the ungual phalanx of central digit (V 18837.17, Fig. 6F).

Measurements See Tables 5–12.

Description IVPP V 18837.1 is a fragmentary maxilla with the P3–M2. The facial crest terminates above the anterior margin of the M1. The preorbital fossa is located above the P3, and the foramen fossa is above the P4. In occlusal view, the center of the posterior margin of

the hard palate is approximately level with the posterior portion of the M2 (Fig. 5C1). On V 18837.4, the major palatine foramen is visible and level with the posterior portion of the M2, whereas the minor palatine foramina are not discernable.

On V 18837.1, the size of the upper cheek teeth gradually decreases from the P3 to M2 (Fig. 5C1). The parastyle is only broadened on the P3–M1, where it is bifid and made up of

Table 5 Mesurements of the lower cheek teeth of *Hipparion* (*Plesiohipparion*) *huofenense* (mm)

		Yegou			Jingle[1)]	Yushe[2)]
		V 18837.2	V 18837.3	V 18837.7	RV 31031	THP10733
p2–p4	L	81.0		82.0		81.0
m1–m3	L	75.5	74.0	67.5	70.5	73.0
p2–m3	L	155	150.0	141.0		154.0
p2	L	32.7		28.7	23.5	29.0
	W	12.5		12.0	17.0	13.1
	doubleknot length	14.0		11.3		13.5
p3	L	26.7		22.4	24.0	23.6
	W	12.2		12.2	17.0	14.2
	doubleknot length	17.0		13.0		14.7
p4	L	24.6		22.8	21.0	22.6
	W	12.3		11.8	16.5	13.0
	doubleknot length	16.4		12.4		14.3
m1	L	22.4		21.0	23.5	21.4
	W	12.3		10.7	16.0	12.0
	doubleknot length	15.0		12.4		13.2
m2	L	23.2		21.5	24.0	22.0
	W	11.0		9.7	15.0	11.9
	doubleknot length	14.0		12.0		13.2
m3	L	30.0		22.0		25.3
	W	10.8		8.5		10.7
	doubleknot length	13.0		10.0		11.9

1) from Teilhard de Chardin and Young (1931); 2) from Qiu et al. (1987).

Table 6 Measurements of the upper cheek teeth of *Hipparion* (*Plesiohipparion*) *houfenense* (mm)

		Yegou				Yushe (Qiu et al., 1987)
		V 18837.5	V 18837.6	V 18837.1	V 18837.4	THP10733
P2	L	33.8	33.8			33.5
	W	22.0	21.8			25.3
	W/L×100	65.1	64.5			75.5
P3	L			27.3		25.0
	W			26.8		24.7
	W/L×100			98.2		98.8
P4	L			25.0		25.0
	W			26.4		25.0
	W/L×100			105.6		100.0
M1	L			21.4	22.4	22.2
	W			25.5	25.3	21.9
	W/L×100			119.2	112.9	98.6
M2	L			22.0	22.8	22.4
	W			22.8	24.3	22.2
	W/L×100			103.6	106.6	99.1
M3	L				25.0	21.8
	W				20.0	19.4
	W/L×100				80.0	89.0

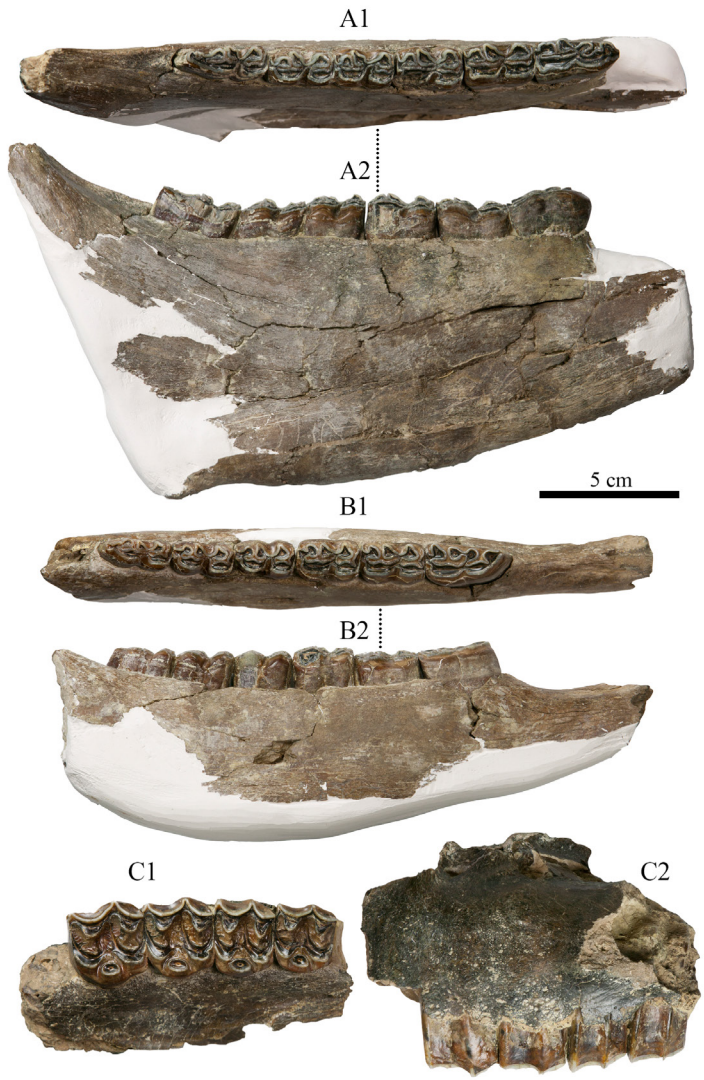

Fig. 5 Fragmentary maxilla and mandibular corpora of *Hipparion* (*Plesiohipparion*) *houfenense* from Yegou A. right mandibular corpus with p2–m3 (IVPP V 18837.3); B. right mandibular corpus with p2–m3 (V 18837.7); C. right maxilla with P3–M2 (V 18837.1); 1. occlusal view, 2. buccal view

two ribs and one median cleft. The anterior rib and median cleft are not developed on the M2. The size of the median cleft gradually decreases from the P3 to M1. The mesostyle is only slightly elongated on the P3–M1, but not on the M2. The labial wall of the paracone and the metacone is labially concave, and their lingual walls are lingually convex. The angle between the anterior lingual and posterior lingual walls tend to become smaller from the P3 to M2, but all less than 90°. The anterolabial corner of the postfossette extends more labially than the posterolabial corner of the prefossette on the cheek teeth. The hypoconal groove is shallow, and the hypoconal constriction is distinct. The counting of enamel plications in the form of "anterior wall of the prefossette.posterior wall of prefossette-anterior wall of postfossette.

posterior wall of postfossette/pli caballin" is as follows: P3 = 6.10-7.2/4, P4 = 6.8-6.2/3, M1 = 6.7-6.1/1, M2 = ?-3.1/1. The protocone length index (= protocone length/tooth length×100) is as follows: P3 = 23.8, P4 = 29.2, M1 = 35.0, M2 = 27.3. The protocone width/length index (= width/length×100) is as follows: P3 = 70.8, P4 = 64.4, M1 = 61.3, M2 = 70.0.

The size of V 18837.4 is small. The major palatine foramen lies between the M2 and M3. The parastyle is elongated on the M1 but not bifid. It is not elongated on either the M2 or the M3. Its extent of labial protruding gradually decreases from the M1 to M3. The hypoconal groove is shallow, and the hypoconal constriction is distinct. The counting of enamel plications is as follows: M1 = 6.8–3.1/3, M2 = 6.9–3.2/2, M3 = 5.8–4.2/2. The protocone length index: M1 = 34.1, M2 = 31.8, M3 = 19.7. The protocone width/length index: M1 = 69.7, M2 = 68.6, M3 = 57.6.

V 18837.5 and V 18837.6 are the left and right P2, respectively. The anterostyle is not inflated. The size of the hypoconal groove is comparable to that of the hypoconal constriction. The left P2 is slightly smaller. The mesostyle extends more labially. The protocone is relatively short and small. Its lingual margin is concave lingually. The protocone of the right P2 is long and robust. Its lingual margin is straight but anterolabially oblique. The counting of enamel plication of the two teeth is 4.2–3.1/1 and 3.4–4.2/2, respectively. The protocone length index: 21.5 and 25.1. The protocone width/length index: 61.6 and 72.9.

Mandible and mandibular cheek teeth (Fig. 5A–B): The larger left and right mandibular corpora should belong to the same individual. Only the right horizontal ramus is relatively complete (V 18837.3, Fig. 5A). The depth beneath the p2 on the lingual side is 72.0 mm. The depth between the p4 and m1 is 88.5 mm. The depth beneath the m3 is 98.0 mm.

The p2 is slightly longer than the p3. The paraconid is robust. The anterior lobe of the double-knot (the metaconid) is rounded and about half the size of the posterior lobe (the

Table 7 Measurements of the humerus of *Hipparion* (*Plesiohipparion*) *houfenense* (mm)

	Yegou		Jingle[1)]	Yushe[1)]
	V 18837.8	V 18837.9	RV 31036	THP10106
distal maximal breadth	56.5	56.3	75.0	75.0
distal breadth at trochlea	50.5	49.4	76.0	75.0
trochlear depth at sagittal groove	28.2	30.2	39.0	37.0
distal maximal depth	37.5	37.6	51.0	51.0
distance between posterior margins of lateral ligment pit and lateral epicondyle	7.0	7.2	11.0	11.0

1) from Qiu et al. (1987).

Table 8 Measurements of the metacarpal III of *Hipparion* (*Plesiohipparion*) *houfenense* (mm)

	Yegou (V 18837.10–11)	Yushe (range, mean, number) [1)]
proximal articular breadth	43.3	44.0–52.6, 49.1, 19
proximal articular depth	28.7	32.0–35.8, 34.3, 20
diaphysis minimal breadth	32.2	28.9–36.4, 32.8, 23
diaphysis depth at minimal breath	25.8	24.8–31.0, 27.2, 23
distal maximal articular breadth	40.0	41.4–47.2, 43.9, 20
distal maximal supra-articular breadth	42.0	41.7–46.7, 43.4, 20
distal maximal depth of the keel	35.2	34.2–38.3, 36.1, 22
distal minimal depth of the medial condyle	29.6	27.1–32.7, 30.0, 22

1) from Qiu et al. (1987).

metastylid). The double-knots of the p3 and p4 are triangular and equal in size. The double-knots of m1–3 are also triangular, but the metaconids gradually become bigger than the metastylid from the m1 to m3. The isthmus is short on the p2–4 but distinct. It is not developed on m1–3. The lingual flexid is U-shaped. It is the shallowest on the p2, and gradually becomes deeper afterwards. The ectoflexid is also shallow on the p2, but gradually becomes deeper afterwards. The pli caballinid and the pli antecaballinid are distinct on p3–m3 of the smaller specimen V 18837.7 (Fig. 5B), whereas only the pli antecaballinid is distinct on the larger specimen V 18837.3 (Fig. 5A). There are no pli caballinid and pli antecaballinid developed on the p2 of either specimen. The protostylid is developed on both specimens, but the pli hypostylid and the ectostylid are not developed. On V 18837.7, the m3 is slightly longer than the m2, which is similar to the holotype RV 31031 from Jingle. The m3 of V 18837.3 is distinctly larger than the m2 and similar to THP10733 from Yushe.

Humerus (V 18337.8, Fig. 6D): The lateral supracondylar crest extends posteriorly and distally to the posterior margin of the lateral ligament fossa, weakens medially, and terminates behind the articular surface of the lateral epicondyle. The distal breadth of the articular surface of the medial condyle (33.0 mm) is about twice of that (16.0 mm) of the lateral condyle. The

Table 9 Measurements of the calcaneus of *Hipparion* (*Plesiohipparion*) *houfenense* from Yegou (mm)

	V 18837.14
maximal length	>95.0
maximal articular length	52.5
breadth at calcaneal tuberosity	21.0
distal maximal breadth	50.0
minimal breadth	40.0
proximal maximal depth	42.0
distal maximal depth	41.0
medial talar articular breadth/depth	18.0/36.0
lateral talar articular breadth/depth	23.0/36.0
metatarsal articular breadth/depth	13.0/35.0

Table 10 Measurements of the talus of *Hipparion* (*Plesiohipparion*) *houfenense* (mm)

	Yegou (V 18837.13)	Jingle (RV 31032)[1)]	Yushe (THP10731)[1)]
maximal length	56.0	62.9	61.2
maximal diameter of medial condyle	57.3	60.1	61.5
maximal breadth	59.0	63.2	63.0
breadth of trochlea (at the apex of each condyle)	28.0	30.0	29.3
distal articular breadth	47.0	51.5	48.7
distal articular depth	32.0	39.5	35.7
maximal medial depth	49.5	51.0	62.5

1) from Qiu et al. (1987).

Table 11 Measurements of the metatarsal III of *Hipparion* (*Plesiohipparion*) *houfenense* (mm)

	Yegou (V 18837.15)	Yushe (range, mean, number)[1)]
proximal articular breadth	46.2	44.0–50.6, 47.8, 18
proximal articular depth	33.0	35.6–40.0, 37.7, 19
minimal breadth (near the middle)	29.0	26.6–34.0, 31.7, 24
diaphysis depth at minimal breadth	27.5	27.8–33.9, 31.5, 24

1) from Qiu et al. (1987).

trochlear depth on the medial condyle side (37.0 mm) is about 1.3 times of that (28.0 mm) on the lateral condyle side. The sagittal crest between the medial and lateral condyles is rounded anteriorly but sharp posteriorly and extends posterolaterally.

Mc III (V 18837.10, Fig. 6A): The proximal articular surface is made up of the smaller lateral articular facet with the unciform (os carpale IV) and the larger medial articular facet with the magnum (os carpale III). The two facets meet at an obtuse angle. The ratio between the depth and the width of the surface is about 4:6. The articular facet with the magnum is flat but slightly tilts medially. There is a distinct protruding point at the posteromedial corner. The posterior margin of the facet is straight and parallel to the volar surface. The articular facet with the unciform is rectangular, concave at the anterior portion, and flat at the posterior portion. It tapers posteriorly. The ridge where the two factes intersect is sharp anteriorly and blunt posteriorly. There is another articular facet with Mc IV lateral to the articular facet with the unciform. It is divided into the wider anterior part and the narrower posterior part, which are connected to each other. The diaphysis is wide and dorsovolarly compressed. There is a longitudinal groove tapering distally on the volar surface. The depression above the distal articular surface on the dorsal side is not well defined. The attachment tuberosity for the collateral ligaments is situated anteriorly, and in lateral view, the contact surface for the lateral phalanges above it bends anteriorly. The sagittal crest of the distal articular surface is widened and rounded at the dorsal end but is sharp and extends proximally at the volar end. A ridge extends proximally from the volar end of the sagittal crest and separates the distal portion of the diaphysis into two approximately equal depressions on the volar side. The distal articular surface is divided by the sagittal crest into the wider lateral part and the narrower medial part. The depth of the lateral part is greater than that of the medial part.

Mc II: The proximal half is preserved. The volar side of the diaphysis is concave. The depth of the diaphysis is greater than that of the contact surface with the Mc III. The proximal articular surface is flat, perpendicular to the diaphysis, and slightly higher than the proximal articular surface of the Mc III when it is in anatomical position. There are two separated articular facets with the Mc III on the medial side and one with the Mc I on the lateral side.

Talus (V 18837.13, Fig. 6E): The talus is asymmetrical. The lateral condyle is distinctly

Table 12 Measurements of the ungual phalanx of *Hipparion* (*Plesiohipparion*) *houfenense* (mm)

	Yegou (V 18837.17)	Yushe (THP30959)[1)]
anterior length	52.4	58.7
length from the posterior edge of the articular surface to the tip of the phalanx	51.2	65.9
angle between the sole and the dorsal line	≥45°	44°
maximal breadth	53.3	70.7
maximal breadth of flexor surface	36.7	43.4
maximal depth of flexor surface	19.0	24.0
maximal height	36.3	60.0
articular breadth/depth	34.5/21.0	

1) from Qiu et al. (1987).

wider than the medial condyle, but the depth of the former is distinctly less than the latter. The slope of the medial wall of the lateral condyle is gentle. The dorsoplantar distance between its distal end and the distal articular facet is 10.0 mm. The medial wall of the medial condyle is nearly vertical and extends posteriorly about half of the depth of the body. The distal portion of medial wall does not bend medially. The depth at the median groove of the trochlea is

Fig. 6 Limb bones of *Hipparion* (*Plesiohipparion*) *houfenense* from Yegou
A. proximal portion of left Mc III (IVPP V 18837.10: 1. proximal view, 2. anterior view);
B. proximal portion of right Mt III (V 18837.15: 1. proximal view, 2. anterior view);
C. proximal portion of right Mt II (V 18837.16: anterior view);
D. distal portion of right humerus (V 18837.8: posterior view); E. right talus (V 18837.13: anterior view);
F. ungual phalanx of the central digit (V 18837.17: anterior view);
G. right calcaneus (V 18837.14: 1. lateral view, 2. medial view)

about 70% of that of the lateral condyle. There are 4 articular facets with the calcaneus. The medial facet is a long strip in shape, with its long axis proximodistally oriented. The medial margin is convex, whereas the lateral margin is concave. It is 31.0 mm long and 13.5 mm wide. The lateroproximal facet is a transverse and anteriorly convex curved surface and it is mediodistally oriented. The proximolateral margin intersects with the lateral wall of the lateral condyle. The tounge-shaped facet or lateral facet is small, with a pointed proximal margin and a rounded distal margin. The proximodistal dimension is 9.0 mm, and the mediolateral dimension is 5.0 mm. The lateroproximal facet and the lateral facet are not connected with each other. The laterodistal facet is rectangular, anteriorly wider, and posteriorly narrower. The anteroposterior dimension is 10.0 mm, and the proximodistal dimension is 7.0 mm. The distal facet is triangular. A concave rough surface medially stretches into the facet from the middle part of its lateral margin and terminates behind the distal end of the medial condyle. The width of the distal facet is 45.5 mm, and the depth is 34.0 mm. The posterior pointed protrusion exists, but it is weak. The medial proximal protuberance is distinct and posterior to the proximal end of the medial condyle of the trochlea. It extends posteriorly about 6.0 mm. The distal protuberance is relatively strong and protrudes medially. The two protuberances are connected by a shallow ridge between them.

Calcaneus (V 18837.14, Fig. 6G): The calcaneal tuberosity is damaged. The medial articular facet is a long strip in shape and slightly concave. Its posteromedial margin leans medially. Its length is 35.2 mm, and its width is 16.3 mm. This facet corresponds to the medial articular facet of the talus. The proximolateral articular facet is nearly circular in outline. It is divided into two parts perpendicular to each other by a transverse ridge. Its width is 22.3 mm, and its depth is 21.0 mm. The tongue-shaped or lateral articular facet is rectangular and connected with the proximolateral articular facet, with a width of 8.4 mm and a length of 16.2 mm. The distolateral articular facet is trapezoid in outline, and the distolateral margin is pointed with a dorsodistal dimension of 20.0 mm and a plantarodistal dimension of 7.2 mm. The distal articular facet is laterally wider and medially narrower. The plantaromedial third of the facet suddenly shrinks. In lateral view, the angle between the lateral margin of the distal articular facet and the dorsodistal margin beneath the tongue-shaped facet is acute.

Mt III (V 18837.15, Fig. 6B): Only the proximal portion is preserved. The depth is slightly less than the breath at the middle of the diaphysis. The plantar side is distinctly concave. The vascular impression is distinct on the lateral side of the proximal Mt III, which intersects with the dorsal margin of the diaphysis about 3 cm beneath the proximal articular facet at an angle of about 45°. Then it runs distally along the lateral margin of the Mt IV. There is a concave non-articular rough surface that extends anteromedially into the center of the proximal articular facet from the plantarolateral corner. The proximal articular surface consists of the medial articular facet with the small cuneiform (os tarsalia I+II), the middle articular facet with the big cuneiform (os tarsale III), and the lateral articular facet with the cuboid (os tarsale IV). The articular facet with the small cuneiform is the smallest among them. It is

semi-circular and intersects with the facet with the big cuneiform at an angle larger than 90°. The articular facet with the big cuneiform is the largest and horseshoe-shaped. Both wings of the facet as well as the plantar and dorsal ends are prominent. The facet intersects with the articular facet with the cuboid at an angle of about 120°. The latter is relatively large, flat and rectangular. There are 2 isolated articular facets on the medial and lateral sides of the proximal articular surface, articulating with the Mt II and Mt IV respectively.

Ungual phalanx of the central digit (V 18837.17, Fig. 6F): The angle between the sole and the dorsal line is about 45°. The rough area for the insertion of the flexor digitorum profundus is distinct and large on the posterior surface where there is a protuberance in the center. The articular facet is semi-circular. The anterior margin is slightly convex, and the posterior margin is straight. It is made up of two concave surfaces: the lateral one and the medial one.

Comparisons and discussion *Hipparion houfenense* or its conformis species have been known from Jingle, Shanxi (Teilhard de Chardin and Young, 1931), Pucheng, Shaanxi (Jen, 1965, =*Hipparion* cf. *huofenense*), Huoxian, Shanxi (Tong et al., 1975, =*Hipparion* cf. *huofenense*), Yushe, Shanxi (Qiu et al., 1980), Weinan, Shaanxi (Xue, 1981), Yuxian, Hebei (Tang and Ji, 1983, = *Hipparion* cf. *huofenense*), Lingtai, Gansu (Zhang et al., 1999: p2–m3 length, 145.5 mm). Among them, the material from Huoxian has been excluded from *H. houfenense* (Qiu et al., 1980); the material from Weinan has been assigned to *H.* (*Proboscidipparion*) *pater* (Qiu et al., 1987); the material from Pucheng has been assigned to *H.* (*Plesiohipparion*) *huangheense* (Qiu et al., 1987)

The smaller mandible from Yegou (V 18837.7) is close to the specimens from Jingle, whereas the larger mandibles (V 18837.2–3) are close to the Yushe specimens. The main difference between these forms lies in that m3 of the former lacks an extra posterior lobe. The size of the Yegou upper cheek teeth is comparable to the Yushe specimens, but the protocone length index is greater, which means the protocone of the former is more rounded than that of the latter. The Mc III, Mt III and the ungual phalanx from Yegou are all smaller than the Yushe specimens, and the humerus and the talus are also smaller than the specimens from Jingle and Yushe. Due to the limited sample size, the smaller dimensions probably do not indicate primitiveness but rather individual variations. For example, the specimens with greater protocone length index represent aged individuals, whereas the smaller limb bones represent young individuals.

***Dicerorhinus* sp.**

(Fig. 7)

Material Proximal portion of the left Mc II (IVPP V 18838.1, Fig. 7D), distal portion of the left Mc III (V 18838.2, Fig. 7A), distal portions of 2 left Mt IIs (V 18838.3, Fig. 7B; V 18838.4), distal portions of 2 left Mt IVs (V 18828.5; V 18838.6, Fig. 7C), right patella (V 18838.7, Fig. 7E), distal portion of the left radius (V 18838.8, Fig. 7G), left calcaneus (V 18838.9, Fig. 7F), proximal portion of the left calcaneus (V 18838.10).

Measurements See Table 13.

Description IVPP V 18838.8 is the distal portion of a radius (Fig. 7G). The diaphysis is robust and anteroposteriorly compressed. The medial margin is flat and thick, while the lateral margin is compressed and thin. The anterior surface is slightly convex, and the posterior surface is slightly concave. The distal outline is triangular. There is a tuberosity with a rough surface on the lateral side, which contributes to the maximal distal breadth. The anterior portion of the distal articular facet is concave, whereas the posterior portion is convex. The distal articular facet is divided into the larger medial part and the smaller lateral part by a low ridge. The lateral part articulates with the ulnar carpal, and the medial part articulates with the radial carpal. The medial articular facet with the radial carpal is semi-circular and intersects with the articular facet with the ulnar carpal approximately at a right angle.

Only the proximal half of the Mc II is preserved (V 18838.1, Fig. 7D). The proximal outline is triangular. On the medial side, there is a triangular rough surface beneath the proximal articular surface. Posterior to this surface, there is a long bar-like protuberance. There is another protuberance medial to the surface. The articular facet with the trapezium (os carpale I) is the largest and it is semi-circular. It is concave in the middle and separated from the long strip-like and anteroposteriorly oriented articular facet with the trapezoid (os carpale II) by a sharp ridge. The articular facet with the Mc III is oval in shape with its major axis anteroposteriorly oriented. It is separated from the facet with the trapezoid by a proximally convex low ridge.

Only the distal half of the Mc III is preserved (V 18838.2, Fig. 7A). The diaphysis is broad and dorsovolarly com-pressed. The lateral side of the bone is rougher than its medial side. The proximal margin of the distal articular facet on the dorsal side is proximally convex. The sagittal crest is not seen on the dorsal side, but it is strong on the volar side where it extends proximally and connects to a large tuberosity.

The patella is complete (V 18838.7, Fig. 7E). It is a large sesamoid bone that is robust and rectangular in outline. The dorsal surface of the bone, for insertion of tendons, is convex and rough. The articular surface with the patellar surface of the femur is also rectangular. There is a broad and rounded ridge dividing the surface into the lateral and the medial parts.

Calcaneus: V 18838.9 is an incomplete calcaneus with only the tuberosity broken off (Fig. 7F). V 18838.10 preserves only the tuberosity and part of the body. Its body is stout. The tuberosity is robust, and its posterior surface is rough. Curved ridges can be seen on the mediodistal margin of the tuberosity. The lateral side of the body proximal to the cochlear process is slightly convex, but the medial side is slightly concave. Both sides are smooth. The articular surface with the talus is divided into two parts by the calcaneal groove. The lateral facet is circular and convex, and the medial facet is tadpole-shaped and concave. The calcaneal groove is deep and extends first distally then distolaterally beneath the lateral facet, where it becomes shallow and merges with the distal margin of the lateral facet. The distal articular facet with the cuboid (os tarsalia IV+V) is semi-circular, concave and intersects with the medial facet with the talus at an angle slightly larger than 90°.

Table 13 Limb bone measurements of selected species in *Dicerorhinus*, *Elasmotherium* and *Coelodonta* (mm)

	Yegou	Hajnáčka	Hundsheim	Nihewan	
	Dicerorhinus sp.	*D. megarhinus*[1)]	*D. etruscus*[1)]	*E. peii*[2)]	*C. nihowanensis*[3)]
Radius					
distal maximal breadth	110.0	105.0–116.0	100.5		
distal maximal articular breadth	93.0	87.5–99.0	73.0–73.8		82.0–115.0
distal maximal depth	67.0	75.0	59.0		
distal maximal articular depth	47.5	55.0			
breadth of articular surface with magnum	44.0	42.0–47.0			
breadth of articular surface with scaphoid	47.0	62.0			
Metacarpal II					
proximal maximal breadth	58.5	50.0–55.0	42.0–43.0		39.0
proximal maximal depth	48.0	40.0–57.0			
breadth at the middle of diaphysis	41.0	38.0–41.5			
depth at the middle of diaphysis	24.0	22.0–32.0			
Metacarpal III					
breadth at the middle of diaphysis	55.0	52.0–65.2	48.5–52.6	69.4–76.0	
depth at the middle of diaphysis	25.0	23.4–24.0	19.0–24.0	30.0–35.8	
distal maximal breadth	65.5			91.8–105.7	53.0
distal maximal articular breadth	51.0	51.0–59.5	44.0–50.5	77.0–87.2	
distal maximal articular depth	54.0	49.0–51.0	51.0		
Patella					
sagittal length	124.0	130.0	108.2		
breadth	101.5	110.0	86.0		
maximal depth	75.0	78.0	52.0		
articular sagittal length	95.0	83.0			
articular breadth	91.0	94.0			
Calcaneus					
length	113.0				
articular length	92.0				
breadth at calcaneal tuberosity	41.0				61.3
maximal breadth	90.0				
depth at calcaneal tuberosity	70.0				108.7
distal maximal depth	91.5				
tarsal articular breadth	31.0				
tarsal articular depth	54.0				
medial talar articular breadth	42.0				
talar articular depth	77.0				
lateral talar articular breadth	44.0				
lateral talar articular depth	42.0				
Metatarsal II					
breadth at the middle of diaphysis	44.0	32.0–37.0	30.0	54.5	
depth at the middle of diaphysis	31.0	27.0–33.0	26.0	29.3–34.5	
distal maximal breadth	50.0, 45.0	49.0	39.0		31.0
distal maximal articular breadth	55.0, 47.5	41.0	35.0		
distal maximal articular depth	62.0, 53.5	43.0	45.0		
Metatarsal IV					
breadth at the middle of diaphysis	34.0	31.0–39.0	31.0		
depth at the middle of diaphysis	29.0	23.0–32.0	24.0		
distal maximal breadth	43.0, 49.0	46.0–55.0	38.7		33.0
distal maximal articular breadth	46.0, 52.0	43.0–47.0	36.5		
distal maximal articular depth	53.0, 58.0	43.0–49.0	41.2		

1) from Fejfar (1964); 2) from Deng and Zheng (2005); 3) from Teilhard de Chardin and Piveteau (1930).

Fig. 7 Limb bones of *Dicerorhinus* sp. from Yegou
A. distal portion of left Mc III (IVPP V 18838.2: anterior view); B. distal portion of left Mt II (V 18838.3: anterior view); C. distal portion of left Mt IV (V 18838.6: anterior view); D. proximal portion of left Mc II (V 18838.1: anterior view); E. right patella (V 18838.7: 1. anterior view, 2. posterior view); F. left calcaneus (V 18838.9: anterior view); G. distal portion of left radius (V 18838.8: anterior view)

There are two Mt IIs, with one being larger than the other. Only the distal protion is preserved (V 18838.3, Fig. 7B). The depth of the diaphysis is larger than the breadth. The medial margin is relatively flat and thicker than the lateral margin. The medial surface is rough. The maximal breadth of the distal articular facet is at the midpoint of the depth. The sagittal crest is only prominent on the plantar side. The articular surface is higher than the diaphysis surface on the dorsal side of the larger specimen, and at the same level on the smaller specimen. The sagittal crest is robust and distinctly proximally exceeds the articular surface on the plantar side of the larger specimen, but only slightly on the smaller specimen. The difference in size and morpholoty probably reflects not only variation, but also interspecific distinction.

There are two Mt IVs as well. One is larger, and the other is smaller. Only the distal portion is preserved (V 18838.6, Fig. 7C). The morphology is basically the same as that of the Mt II.

Comparisons and discussion Three rhinocerotid species have been known from the Early Pleistocene deposits of the Nihewan Basin, including the distinctly small-sized *Dicerorhinus mercki* (=*Stephanorhinus kirchbergensis*), medium-sized *Coelodonta nihowanensis*, and large-sized *Elasmotherium peii* (Teilhard de Chardin and Piveteau, 1930; Deng and Zheng, 2005: *Elasmotherium caucasicum*; Tong et al., 2014). Among them, only the limb bones of the the latter two species have been unearthed (Teilhard de Chardin and Piveteau, 1930; Deng and Zheng, 2005). In terms of the measurements (Table 13), the sizes of the Mc III, calcaneus, and Mt II described here are distinctly smaller than the corresponding elements of Early Pleistocene *Elasmotherium peii* from the same basin. The size of the radius is similar, but that of Mc II–III and Mt II, IV is distinctly greater than Early Pleistocene *Coelodonta nihowanensis* from the same basin. Although *Dicerorhinus mercki* is also known from the Nihewan Basin, there are only limb bones from Yegou, which lack decisive

diagnostic morphological characters. Consequently, the new material is temporarily identified as *Dicerorhinus* sp.

A Mc II that is close to the Yegou specimen is known from the red clay layer of Renjiagou, Lingtai, Gansu (Zhang et al., 1999: Rhinocerotidae gen. et sp. indet.). The proximal length/width is 55.0 mm/41.0 mm, and the minimal breath/depth of the diaphysis is 39.5 mm/23.3 mm. The magnetostratigraphic age of the horizon is 3.5–3.4 Ma (Sun et al., 1998; Zhang et al., 1999).

The size of the Yegou specimen is also very close to that of the *Dicerorhinus megarhinus* (Christol, 1835) from Hajnáčka, southern Slovakia (Fejfar, 1964). Based on the coexisting *Mimomys hajnackensis* Fejfar, 1961, its geological age should be Early Villanyian, > 3 Ma (Repenning et al., 1990).

Gazella blacki Teihard de Chardin & Young, 1931

(Fig. 8)

Material Left horn core with the pedicle and partial frontal bone but without the tip (IVPP V 18839.1, Fig. 8B), left horn core without the pedicle but with the tip slightly damaged (V 18839.2), 1 left and 1 right fragmentary mandibular corpora with the p2–m3 (V 18839.3; V 18839.4, Fig. 8A), fragmentary right mandibular corpus with the p2 alveoli and the p3–m3 (V 18839.5), fragmentary right mandibular corpus with the p3–p4 (V 18839.6), fragmentary right mandibular corpus with the m3 (V 18839.7).

Measurements See Table 14.

Description V 18839.1 (Fig. 8B) is a fragmentary horn core with the dorsal half missing and a small portion of frontal bone preserved at the pedicle. The supraorbital foramen can be seen anterior to the pedicle of the core. The postcornual fossa is deep and oval on the lateral side of the pedicle. The horn core slightly bends caudally. There are coarse and parallel longitudinal ridges (or grooves). Judging from the suture preserved on the medial side, the minimal distance between the pedicles is about 2.4 cm. The horn core extends caudolaterally. The other specimen does not have the frontal bone preserved, and the tip is slightly damaged (V 18839.2). Its curvature is similar to that of V 18839.1. Although the rostral surface is damaged, it seems that the longitudinal ridges (or grooves) are not as coarse as that of V 18839.1.

All mandibular specimens are incomplete. The length of p2–p4 is 38% of that of the lower cheek teeth row, but greater than that of m2–m3. The p2 is single lobed with a pointed protoconid and two roots. The p3 and p4 both have anterior, middle, and posterior valleys. The middle and posterior valleys can both reach the labial side. The metaconid and the paraconid are not fused completely on the p4. The protoconid is pointed. The morphology of lower molars is similar to that of other gazelles, but the goat fold is present anterolaterally in young individuals.

Comparisons and discussion The material described in this paper is slightly larger than *Gazella blacki* from Xiaohongao, Hefeng and Renjiagou, Lingtai, and distinctly smaller than *G. sinensis* from the Nihewan Basin (Table 14). The average ratios of the p2–p4 length to the p2–m3 length in percentage for these three forms are 38.2% (Xiaohongao), 36.2% (Renjiagou), and 35.3%

(Nihewan) respectively. The material here is therefore closer to *G. blacki* than to *G. sinensis*.

When studying the gazelle fossils from North China, especially Yushe, Chen (1997a,b) pointed out that *Gazella blacki* is a valid species, and it is a typical form for the Late Pliocene of North China. The magnetostratigraphic age provided by Chen (1994) is ca. 3 Ma.

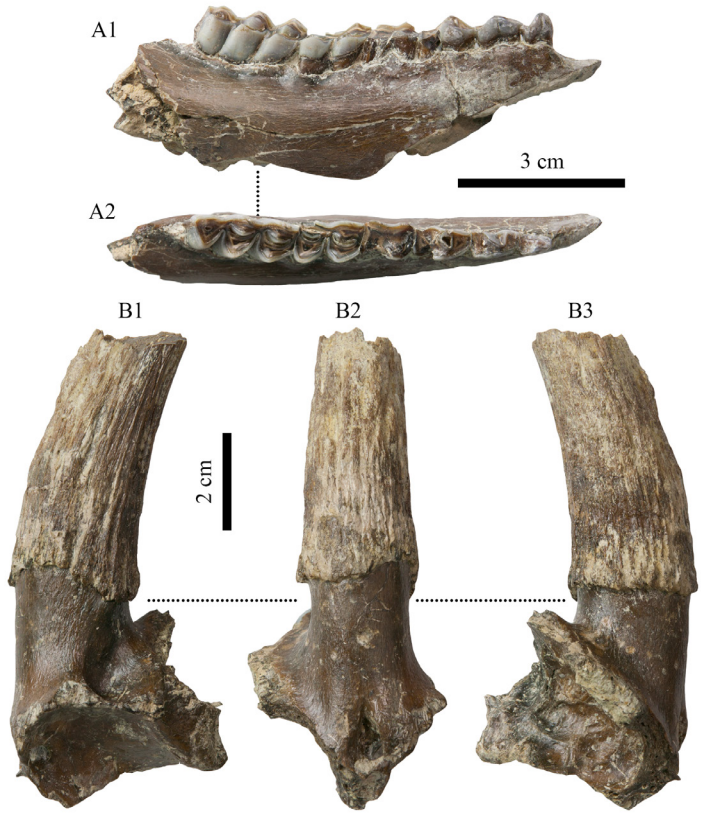

Fig. 8 Selected dentition and horn core of *Gazella blacki* from Yegou
A. fragmentary right mandibular corpus with p2–m3 (IVPP V 18839.4: 1. buccal view, 2. occlusal view; 3 cm scale bar);
B. fragmentary left horn core (V 18839.1: 1. lateral view, 2. anterior view, 3. medial view; 2 cm scale bar)

Table 14 Measurements of the horn core and cheek teeth of *Gazella blacki* and *G. sinensis* (mm)

	G. blacki			*G. sinensis*
	Yegou	Hefeng[1)]	Rengjiagou[2)]	Nihewan[3)]
	range, number			
length of horn core	~100.0	~88.0		
rostrocaudal diameter of horn core base	28.2–29.4, 2	23.0–25.5, 2	24.8	36.0–47.0, 4
breadth of horn core base	23.6–24.7, 2	20.5–22.0, 2	22.5	28.0–36.0, 4
p2–m3	65.3–65.4, 2	62.5–65.0, 3	68.6	65.0–78.0, 3
p2–p4	24.9–25.0, 2	22.0–24.5, 3	24.5	22.0–28.0, 3
p2 length	6.0–6.3, 2	5.2–6.8, 3		
p3	7.8–9.0, 3	7.1–8.9, 3		
p4	10.4–10.6, 3	8.7–9.5, 3		

1) from Chen (1994) and Teilhard de Chardin and Young (1931); 2) from Zhang et al. (1999); 3) from Teilhard de Chardin and Piveteau (1930).

Gazella cf. *G. blacki* also occurs in many Early Pleistocene faunas, such as Wenxi, Houma, (Tang, 1980a), Xihoudu, Ruicheng (Chia and Wang, 1978), Xicun, Tunliu, Shanxi (Zong et al., 1982), and Longdan, Dongxiang, Gansu (Qiu et al., 2004). In this regard, *G. blacki* is probably a long-lasting species spanning from the Late Pliocene to Early Pleistocene.

Axis shansius Teilhard de Chardin & Trassaert, 1937

(Fig. 9)

Material Antler fragment (IVPP V 18841.1, Fig. 9A), fragmentary right maxilla with the P2–M3 (V 18841.2, Fig. 9B), the right P3 (V 18841.3), distal portion of the right radius (V 18841.4, Fig. 9C), distal portion of the left tibia (V 18841.5, Fig. 9D), 1 left and 1 right tali (V 18841.6, Fig. 9E; V 18841.7), proximal portions of 2 Mt III-IVs (V 18841.8, Fig. 9F; V 18841.9).

Measurements See Table 15.

Description The antler (V 18841.1, Fig. 9A) is fragmentary. Only the portion where the

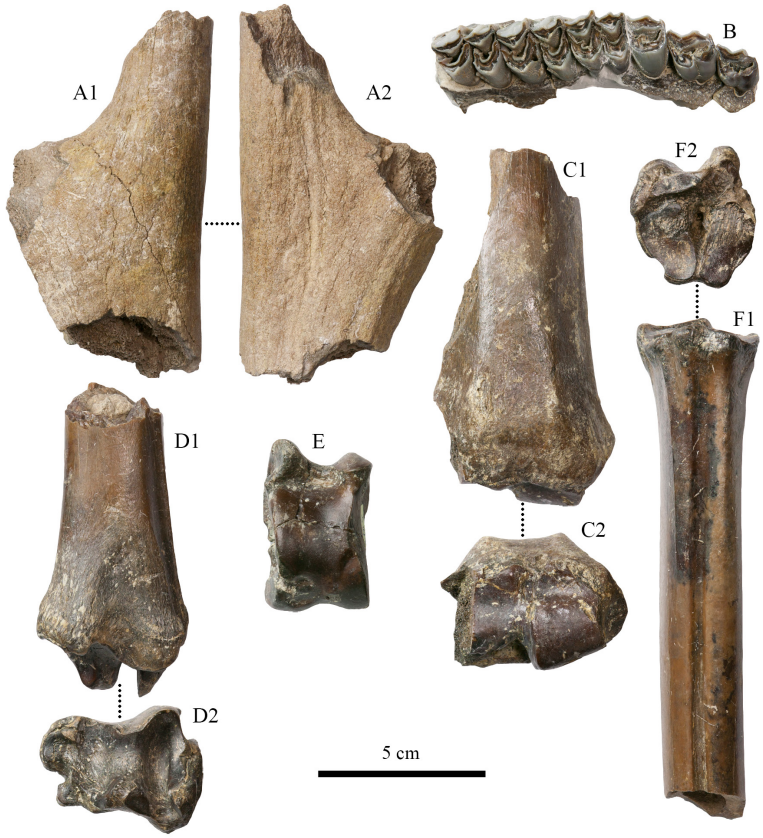

Fig. 9 Antler, upper cheek teeth, and limb bones of *Axis shansius* from Yegou
A. antler fragment (IVPP V 18841.1: 1. lateral view, 2. medial view); B. fragmentary right maxilla with P2–M3 (V 18841.2: occlusal view); C. distal portion of right radius (V 18841.4: 1. anterior view, 2. distal view); D. distal portion of left tibia (V 18841.5: 1. posterior view, 2. distal view); E. left talus (V 18841.6: posterior view); F. proximal portion of left Mt III–IV (V 18841.8: 1. anterior view, 2. proximal view)

Table 15 Measuements of antlers, limb bones and cheek teeth of *Axis shansius* and *Cervus* sp. (mm)

		A. shansius			*Cervus* sp.
		Yegou	Yushe (type, THP27726)[1)]	Guide[2)]	Jingle[3)]
P2–M3		111.0	99.0		
M1–M3	L	51.5	58.0		
P2–P4		45.3	46.0		
P2		15.5/12.0	18.0/12.0		
P3		15.5/14.0	16.0/15.0		
P4	L/W	12.5/16.0	12.5/16.0		
M1		18.0/17.0	18.0/17.0		
M2		20.5/20.0	19.0/19.0		
M3		21.0/19.5	20.0/16.0		
height of antler base		>80.0 (burr not included)	>60.0 (burr included)	87.0–107.0 (burr included)	
maximal diameter of antler base			43.0		
maximal diameter of burr			56.0	56.0	
maximal diameter of antler base above burr		>45.0	43.0	39.0–41.0	
maximal breadth of distal radius		>57.0			50.0
maximal depth of distal radius		39.0			
maximal breadth of distal tibia		49.5			43.0
maximal depth of distal tibia		38.0			
maximal length of talus		48.0–54.5			52.0
maximal breadth of talus		30.0–34.0			33.5
maximal breadth of proximal metatarsal		35.5–37.0			34.0
breadth at the middle of metatarsal diaphysis		24.5–21.5			

1) from Teilhard de Chardin and Trassaert (1937); 2) from Zheng et al. (1985); 3) from Teilhard de Chardin and Young (1931).

main beam and the brown tine bifurcates is preserved. The lateral side of the main beam is also damaged. The medial surface is concave, and longitudinal grooves and ridges can be seen. The lateral surface is flat, and the grooves and ridges are not as clear. Judging from the longitudinal orientation of the main beam, the angle between it and the brown tine is probably greater than 90°.

Enamel rugosity is distinct on the surface of the upper cheek teeth (V 18841.2, Fig. 9B). Spurs are developed on the buccal side of the crescent crests formed by the protocone and the metaconule. The cingulum is developed on the lingual and medial side. The lingual side of the P2 and P3 is double-lobed, and the protocone and the metaconule are developed. The P4 is single-lobed. The parastyle and the mesostyle are more developed than the metastyle on M1–3. The extent of buccal protruding of the parastyle is greater than that of the metastyle. The length of P2–4 is 88% of that of M1–3.

Only the distal portion of the radius (V 18841.4, Fig. 9C) is preserved, and the lateral side is damaged. The medial articular facet is convex, and the lateral articular is posteriorly positioned and concave.

Only the distal portion of the tibia (V 18841.5, Fig. 9D) is preserved. The articular portion is complete. The articulation with the talus is carried out by two facets. They are two anteroposteriorly oriented parallel concave grooves. The lateral one is wider than the medial one, but the latter one is deeper. The articulation with the lateral malleolus (vestigial distal end

of the fibula) is carried out by two small facets on the lateral side. The anterior one is larger, and the posterior one is smaller. They are separated by a notch.

There are two tali. One is left (18841.6, Fig. 9E), and the other one is right (18841.7). The right one is smaller, but their morphologies are the same.

There are two metatarsals (V 18841.8–9, Fig. 9F) and both preserve only the proximal half. The groove on the dorsal side is narrow and extends distally to a very low position. On the medial side of the proximal end of the groove, there is a distinct vascular impression. The plantar groove is wider. The proximal plantar foramen is located at the proximal end of the plantar groove, and it proximodorsally penetrates the proximal metatarsal and opens at the center of the articular surface with the tarsals.

Comparisons and discussion In terms of the size of the limb bones (Table 15), the Yegou material is very close to *Cervus* sp. from Jingle (Teilhard de Chardin and Young, 1931). In terms of the morphology and size of the antler, the Yegou specimen (V 18841.1) is comparable to Early Pleistocene *Axis shansius* from Zone III of Yushe, Shanxi, but the antler is slightly longer. It is closer to the antler of Late Pliocene *A. shansius* from Guide, Qinghai (Zheng et al., 1985). The dimensions of the upper cheek teeth are also generally consistent with the holotype of *A. shansius*.

***Muntiacus* sp.**

(Fig. 10A)

Material Fragmentary right maxilla with the M2–3 (IVPP V 18840, Fig. 10A).

Measurements M1: length, 10.8 mm, anterior width, 12.3 mm, posterior width, 11.3 mm; M2: length, 10.8 mm, anterior width, 12.0 mm, posterior width, 10.3 mm.

Description It is a small-sized muntjac. The molars are low-crowned. The morphologies of the M2 and M3 are similar. There is strong rugosity on the enamel surface. The protocone is more developed than the hypocone, and the paracone is more developed than the metacone. The parastyle and the mesostyle are more developed than the metastyle. The paracone rib is stronger than the metacone rib. Both teeth are 4-rooted. The only difference is that the M2 is slightly larger than the M3.

Comparisons and discussion The morphology and size of the teeth are consistent with *Muntiacus*. Due to the fact that there is no antler, it is hard to identify it to the species level.

***Paracamelus* sp.**

(Fig. 10B–E)

Material Right M2 (IVPP V 18842.1, Fig. 10C), right M3 (V 18842.2, Fig. 10B), distal portion of the left humerus (V 18842.3, Fig. 10E), manual 4th proximal phalanx (V 18842.4, Fig. 10D).

Measurements See Tables 16–18.

Description The molars (IVPP V 18842.1–2, Fig. 10B, C) are large and anteriorly wider. The sloping of the lingual wall of the molars is gentle, so the flaring of the crown

is not distinct. The protocone and metaconule are nearly equal in size, but the protocone extends more lingually. The parastyle is more developed than the mesostyle. The metastyle is extremely weak or not developed. The paracone rib is more robust than the metacone rib. The shrinking of the posterior lobe of the M3 is more distinct than that of the M2. The metastyle is relatively distinct on the M3.

Only the distal portion of the humerus is preserved (V 18842.3, Fig. 10E). The lateral ligament pit is deep. The distal maximal breadth is located where the lateral epicondylar crest is in contact with the margin of the ligament pit. The medial ligament pit is shallow. There is a robust and short ridge posteroproximal to it. The trochlea of humerus is broader than the

Fig. 10 Specimens of *Muntiacus* sp. and *Paracamelus* sp. from Yegou
A. *Muntiacus* sp. (1 cm scale bar): fragmentary right maxilla with M2–3 (IVPP V 18840: occlusal view);
B–E. *Paracamelus* sp. (5 cm scale bar): B. right M3 (V 18842.2: 1. occlusal view, 2 buccal view);
C. right M2 (V 18842.1: 1. occlusal view, 2. buccal view);
D. manual 4th proximal phalanx (V 18842.4: 1. anterior view, 2. posterior view, 3. proximal view);
E. distal portion of left humerus (V 18842.3: posterior view)

capitulum of humerus. The groove between them is shallow. The anteroproximal margin of the trochlea is more proximally positioned on the medial side. The posteroproximal margin of the trochlea extends proximally into the olecranon fossa. The posterodistal margin of the medial epicondyle meets the posterodistal margin of the diaphysis at an angle slightly less than 90°.

The distal articular surface of the proximal manual phalanx of 4th digit (V 18842.4, Fig. 10D) is damaged, but the length of the bone is measurable. The proximal lateral ligament tuberosity is more prominent than the medial one, but the shape and size of the muscle insertion area on both sides are similar. The proximal articular surface is elliptical in shape. There is a depression at the center of the posterior portion of the surface that divides it into two parts. The lateral part is narrower and higher than the medial part. The distal end is slim and narrow. The ligament tuberosity on both sides is weak.

Table 16 Measurements of upper molars of *Paracamelus* sp. and *P. gigas* (mm)

		Paracamelus sp.		*P. gigas*
		Yegou	Renjiagou (Zhang et al., 1999)	Mianchi (Zdansky, 1926)
M2	length	45.5	42.0	?46.0
	anterior width	35.0	29.7	42.4
	posterior width	33.0		
M3	length	43.0	42.0	55.0
	anterior width	34.5	23.5	43.3
	posterior width	29.0		

1) from Zhang et al. (1999); 2) from Zdansky (1926).

Table 17 Measurements of the humerus of *Paracamelus* sp. from Yegou (mm)

distal maximal breadth	71.0
distal maximal depth	73.0
breadth of olecranon fossa	22.0
medial depth of trochlea	44.0
depth of capitulum	50.0
minimal depth between trochlea and capitulum	37.0

Table 18 Measurements of the fourth proximal phalanx of selected camelins (mm)

	Paracamelus sp. (manual)	*P. gigas* (pedal)			*Camelus ferus*
	Yegou	Zhoukoudian[1)]	Mianchi[2)]	Yushe[3)]	extant
length	127.0	112.0	111.5	106.0–131.0	88.0
proximal breadth	55.0	48.0	44.3	44.0–49.0	44.0
distal breadth	37.0	?38.0	36.8	35.0–43.0	34.0

1) from Young (1932); 2) from Zdansky (1926); 3) from Teilhard de Chardin and Trassaert (1937).

Comparisons and discussion Material of *Paracamelus gigas* known from the Quaternary strata in the Nihewan Basin is limited to one calcaneus and the distal portion of one radius (Teilhard de Chardin and Piviteau, 1930). That of *Paracamelus* sp. from the Late Pliocene strata is also limited to one talus (Tang, 1980b). Yegou is therefore the first locality in the Nihewan Basin that has yielded dental remains.

There is material of maxilla with complete dentition, humerus, talus, and metatarsal known from the Upper Pliocene at Renjiagou, Lingtai, Gansu assigned to *Paracamelus* sp.

(Zhang et al., 1999). The size (M2 and M3 length, 42.0 mm) and morphology (including shrinking posterior lobe, developed parastyle and mesostyle, weak metastyle) are the same as that of the Yegou specimen, but the humerus is neither described nor figured, so it can not be compared with the Yegou specimen.

The phalanx (V 18842.4) from Yegou is distinctly larger than that of *Paracamelus gigas* from Loc. 1, Zhoukoudian (Young, 1932) and Mianchi, Henan (Zdansky, 1926), and even larger than that of extant camels.

3 Composition and age of the Late Pliocene *Hipparion houfenense* fauna in Nihewan Basin

The localities or horizons that yield fossils of large mammals including *Hipparion* are relatively rare in the Nihewan Basin. In addition to Yegou and Laowogou (Cai et al., 2004), there are still the following localities: 1) the red clay layer of Luanshigedagou, Hongya Village, yielding *Hipparion* sp. and *Chilotherium* sp. (Huang et al., 1974: Layer 3); 2) the red clay layer of the "Yuxian Formation" of the upper portion of the Huabaogou section (Layer 3), Xiyaozitou Village, yielding *Postschizotherium* sp., *Viverra* sp., *Hipparion houfenense*, *Gazella blacki*, *Gazella* spp., and *Antispiroides hopeiensis* (Wang, 1982; Li et al., 2008); 3) the red clay layer of the "Huliuhe Formation" of the lower portion of the Huabaogou section (Layer 1), Xiyaozitou Village, yielding *Canis* sp., *Canis multicuspus*, *Nyctereutes sinensis*, *Hipparion* cf. *H. hippidiodus*, *Hipparion* sp., *Palaeotragus* spp., *Gazella blacki*, and *Gazella* sp. (Wang, 1982; Li et al., 2008); and 4) the red clay layer of the Danangou section, Dongyaozitou Village, yielding *Lynx variabilis*, *Nyctereutes* cf. *sinensis*, *Hipparion* cf. *H. houfenense*, *Paracamelus* sp., *Antilospira yuxianensis*, and *Palaeotragus progressus* (Layer 1 of Tang, 1980b and Tang and Ji, 1983; Layer 1–2 of Zheng and Cai, 1991 and Cai et al., 2004, 2013; Li et al., 2008).

If the horizon of the Yegou *Hipparion houfenense* fauna can be correlated to Layer 9 of the Laowogou section (Cai et al., 2004), Layer 1 or 3 of the Huabaogou section (Wang, 1982), and Layer 1 (Tang, 1980b; Tang and Ji, 1983) or Layer 1–2 (Zheng and Cai, 1991; Cai et al., 2004, 2013) of the east cliff section of Danangou, then the large mammals of the Late Pliocene mammalian fauna of the Nihewan Basin should tentatively include at least the following 27 forms:

Canis sp. [-]

Canis multicuspus Wang, 1982 [-] (nomen nudum)

Nyctereutes tingi Tedford & Qiu, 1991

Nyctereutes cf. *N. sinensis* (Schlosser, 1903) [-]

Nyctereutes sinensis (Schlosser, 1903)

Pachycrocuta pyrenaica (Depéret, 1890)

Homotherium sp.

Lynx variabilis Tang, 1980 [+]

Viverra sp. [-]

Hipparion houfenense (Teilhard de Chardin & Young, 1931)

Hipparion cf. *H. houfenense* (Teilhard de Chardin & Young, 1931) [-]

Hipparion cf. *H. hippidiodus* Sefve, 1927 [-]

Hipparion sp. [-]

Dicerorhinus sp.

Chilotherium sp. [-]

Postschizotherium sp. [-]

Muntiacus sp.

Axis shansius Teilhard de Chardin & Trassaert, 1937

Cervus sp. [-]

Gazella spp. [-]

Gazella blacki Teilhard de Chardin & Young, 1931

Antilospira sp. [-]

Antilospira yuxianensis Tang, 1980 [+]

Antispiroides hopeiensis Wang, 1982 [-] (nomen nudum)

Palaeotragus spp. [-]

Palaeotragus progressus Tang & Ji, 1983 [+]

Paracamelus sp.

Although most of these fossils have not been systematically studied (species with [-]) or have only been briefly described (species with [+]) and need further taxonomic revision, their Pliocene age (compared with the classic Early Pleistocene Nihewan fauna) is affirmative. These taxonomic names are tentatively retained here for the following discussion in the sense of the fossil entities they represent, including the unidentified species and nomina nuda. Among them, *Viverra*, *Nyctereutes*, *Dicerorhinus*, *Muntiacus*, *Gazella*, *Axis* are extant genera. There are no extant species. Such a dominant proportion of extinct species is not possessed by any other Early Pleistocene faunas.

The key features of the Late Pliocene *Hipparion houfenense* fauna of the Nihewan Basin represented by the 10 large mammals described here are as follows: 1) the coexistence of *Gazella blacki* and *Hippaion* (*Plesiohipparion*) *houfenense*; 2) the coexistence of *Nyctereutes tingi* and *N. sinensis*; 3) the appearance of *Pachycrocuta pyrenaica*; and 4) the coexistence of *Axis shansius* and *Paracamelus*.

According to the first feature, the age of the fauna is directly comparable to those of the red clay of Layer 1, 3 of the Huabaogou section near Xiyaozitou Village in Yuxian Basin (Wang, 1982), the Jingle red clay of the Renjiagou section, Lingtai, Gansu (Zhang et al., 1999), the red clay of Xiaohongao, Hefeng, Jingle, Shanxi (Teilhard de Chardin and Young, 1931; Chen, 1994), the Mazegou Formation of Yushe, Shanxi (Flynn et al., 1991; Deng and Hou, 2011). According to the second feature, *Nyctereutes tingi* only has Pliocene stratigraphic records in the Yushe Basin (Tedford and Qiu, 1991) and Leijiahe, Lingtai, Gansu (Huang et al., 1993) so far, while the coexistence of *N. tingi* and *N. sinensis* only occurs in the Yushe Basin and

the Nihewan Basin. According to the third feature, *Pachycrocuta pyrenaica* is only known from strata before Villafranchian in France, Spain, and Ukraine (Depéret, 1890; Crusafont and Sondaar, 1971; Adrover et al., 1976; Howell and Petter, 1980), whereas in China, it is only known from the lower Mazegou Formation, the Gaozhuang Formation of Pliocene, and even the upper Mahui Formation of Upper Miocene in the Yushe Basin (Qiu, 1987; Deng et al., 2010; Deng and Hou, 2011). According to the fourth feature, in addition to the Late Pliocene records of *Axis shansius* in Guide, Qinghai (Zheng et al., 1985) and Laowogou, Daodi Village, the Nihewan Basin (Cai et al., 2004), the holotype of this species comes from Zone III of Yushe, Shanxi (belongs to the Lower Pleistocene); *Paracamelus* also has both Pliocene records, such as Danangou, the Nihewan Basin (Tang, 1980b) and Renjiagou, Lingtai (Zhang et al., 1999), and Pleistocene records (Teilhard de Chardin and Piveateu, 1930; Teilhard de Chardin and Trassaert, 1937; Young, 1932). Taken as a whole, the age of the Yegou *Hipparion houfenense* fauna should be the Late Pliocene before 2.6 Ma.

The Mazegou Formation of the Yushe Basin, Shanxi is the horizon yielding the richest fossils of Late Pliocene large mammals, and 65 forms have been currently preliminarily identified (Flynn et al., 1991; Deng and Hou, 2011; Wang et al., 2017), which contains nearly all species of large mammals from Late Pliocene localities in North China. It is therefore a helpful standard to compare with when trying to determine if the age of a fauna is Late Pliocene. For example, the sand layer of Guide and the Leijiahe Formation of Lingtai can be correlated the Mazegou Formation to by sharing *Anancus sinensis*; the Leijiahe Formation can also be correlated to the Mazegou Formation by sharing *Hipparion pater.* Accordingly, based on the combinations of *Nyctereutes tingi–N. sinensis* and *Homotherium* sp.–*Dicerorhinus* sp.–*Paracamelus* sp., the Yegou horizon can also be correlated to the Mazegou Formation.

Nyctereutes tingi, *Pachycrocuta pyrenaica*, *Homotherium* sp., *Hipparion* (*Plesiohipparion*) *houfenense*, and *Gazella blacki* of the Late Pliocene Yegou *Hipparion houfenense* fauna of the Nihewan Basin are more primitive than *N. sinensis*, *Pachycrocuta brevirostris licenti*, *Homotherium crenatidens*, *Hipparion* (*Proboscidipparion*) *sinense*, and *Gazella sinensis* of the Early Pleistocene fauna from the Xiashagou-Nihewan Village area, respectively. Consequently, the age of the former fauna should be older.

In the Nihewan Basin, the localities or horizons that yield common faunal elements with the Yegou *Hipparion houfenense* fauna include the following: 1) Layer 9 of Laowogou, sharing *Hipparion* and *Axis shansius* (Cai et al., 2004); 2) Layer 1 of the east cliff section, Danangou, Dongyaozitou Village, sharing *Hipparion* cf. *H. houfenense* (Tang, 1980b; Tang and Ji, 1983); 3) Layer 1 of Huabaogou, Xiyaozitou Village, sharing *Nyctereutes sinensis* and *Gazella blacki* (Wang, 1982); and 4) Layer 3 of Huabaogou, Xiyaozitou Village, sharing *Hipparion houfenense* and *Gazella blacki* (Wang, 1982). Based on biostratigraphic correlations (Li et al., 2008; Cai et al., 2013), Layer 3 of the Huabaogou section can be correlated to Layer 9 of Laowogou; Layer 1 of Huabaogou can be correlated to Layer 2 of Laowogou; Layer 1 of the east cliff section of Danangou can be correlated to Layer 16–19 of Laowogou. Accordingly,

the horizon of the Yegou *Hipparion houfenense* fauna can be generally correlated to the above horizons, especially Layer 9 of Laowogou.

Presently, the magnetostratigraphic dating results of the horizons of the *Hipparion houfenense* fauna characterized by *Hipparion* (*Plesiohipparion*) *houfenense* and *Gazella blacki* are not completely consistent. The red clay of Xiaohongao, Jingle has been dated to 3 Ma (Chen, 1994). The red clay of Renjiagou, Lingtai has been dated to 3.5–3.4 Ma (Sun et al., 1998; Zhang et al., 1999). The Mazegou Formation has been dated to 3.6–2.6 Ma (Flynn and Qiu, 2013). The fossil layer of the east cliff section, Danangou, Dongyaozitou Village has also been dated to 3.04–2.58 Ma (Liu et al, 2021). It can be inferred from these results that the age of the Yegou horizon should fall within the range of 3.6–2.6 Ma. Only the red clay of Layer 1, 3 of the Huabaogou section is unexpectedly younger, the magnetostratigraphic age of them ranges 1.95–1.77 Ma (Zhu et al., 2007; Deng et al., 2008; Deng, 2011). The most likely reason for this is that depositional hiatus in the Huabaogou section may have been ignored by these investigators. This, once again, proves the importance of the mutual compatibility between biostratigraphy and magnetostratigraphy. For the magnetostratigraphic dating results to be robust, it is necessary to carefully verify if the correlation of polarity chrons to GPTS is compatible with biostratigraphy based on fossils, especially when contradictions arise. If contradictions arise, the results are subject to cautious reinterpretation, as is the case for the results mentioned above.

4 Features of Late Pliocene and Early Pleistocene mammalian faunas (large) in Nihewan Basin

In recent years, many Late Pliocene horizons yielding *Hipparion houfenense* have been discovered in North China, such as Layer 1 (Tang, 1980b; Tang and Ji, 1983) or Layer 1–2 (Zheng and Cai, 1991; Cai et al., 2004, 2013) of the Danangou section, Dongyaozitou Village and Layer 1, 3 of the Huabaogou section, Xiyaozitou Village in the Nihewan Basin (Wang, 1982), Renjiagou, Lingtai (Zhang et al., 1999) and the Leijiahe Formation (Huang et al., 1993) in Lingtai, Gansu, the Mazegou Formation of Yushe (Flynn et al., 1991; Deng and Hou, 2011) and Xiaohongao, Jingle (Zhou, 1988; Chen, 1994) in Shanxi, the sand layer of Guide in Qinghai (Zheng et al., 1985), and so on. The discovery of these Late Pliocene horizons with fossils of large mammals provides us with a better understanding about the general features of the *Hipparion houfenense* fauna in China. It should be noted that *Lynx variabilis*, *Hipparion* cf. *H. houfenense*, *Paracamelus* sp., *Antilospira yuxianensis*, etc. in the "Pliocene–Early Pleistocene transitional mammalian fauna" derived from Layer 1 of the east cliff section of Danangou in the Nihewan Basin (Tang, 1980b; Tang and Ji, 1983) should be Late Pliocene in age (Zheng and Cai, 1991; Cai et al., 2004, 2013). Based on the fossils of large mammals derived from the above horizons, the Late Pliocene mammalian fauna (large) in the Nihewan Basin is characterized by having the following features: 1) few Early Pliocene forms, such as *Nyctereutes tingi* Tedford & Qiu, 1991, *Pachycrocuta pyrenacia* (Depéret, 1890), *Hipparion* cf.

H. hippidiodus Sefve, 1927, and *Palaeotragus* sp.; 2) several species unique to Late Pliocene, such as *Canis multicuspus* Wang, 1982 (nomen nudum), *Lynx variabilis* Tang, 1980, *Hipparion* (*Plesiohipparion*) *houfenense* (Teilhard de Chardin & Young, 1931), *Antilospira yuxianensis* Tang, 1980, *Antispiroides hopeiensis* Wang, 1982 (nomen nudum), and *Palaeotragus progressus* Tang & Ji, 1983; 3) some Late Pliocene–Early Pleistocene transitional forms, such as *Homotherium* sp. (Yegou), *Nyctereutes sinensis* (Schlosser, 1903), *Gazella blacki* Teilhard et Chardin & Young, 1931, and *Paracamelus* sp. (Yegou, Danangou); and 4) no extant species.

In addition to the classic Early Pleistocene Nihewan mammalian fauna (large) with multiple revisions and supplements (Teilhard de Chardin and Piveteau, 1930; Qiu, 1987, 2000), numerous Early Pleistocene horizons yielding fossils of large mammals have been discovered in the Nihewan Basin in recent years, such as the Xiaochangliang site (You et al., 1980; Tang et al., 1981, 1995; Chen et al., 1999; Zhang et al., 2008), the Majuangou site (Wei et al., 2003; Cai and Li, 2004; Cai et al., 2008), the west section of Danangou (Tang et al., 1981; Li, 1984), Layer 3, 5 of the east cliff section of Danangou (Tang, 1980b; Tang and Ji, 1983), and so on. Based on the fossils of large mammals derived from these horizons, the Early Pleistocene mammalian fauna (large) in the Nihewan Basin is characterized by having the following features: 1) few Late Pliocene–Early Pleistocene transitional forms, such as *Zygolophodon* sp. (Danangou), *Nyctereutes sinensis* (Schlosser, 1903), *Crocuta honanensis* (Zdansky, 1924), *Hipparion* sp. (Xiaochangliang, Majuangou, Danangou), *Elasmotherium* sp. (Nihewan Village), and *Postschizotherium chardini* von Koenigswald, 1932; 2) a lot of species unique to the Early Pleistocene, including *Mammuthus trogontherii* Pohlig, 1885, *Canis chiliensis* Zdansky, 1924, *Canis* c. var. *palmidens* Teilhard de Chardin & Piveteau, 1930, *Eucyon minor* (Teilhard de Chardin & Piveteau, 1930), *Erictis pachygnatha* (Teilhard de Chardin & Piveteau, 1930), *Meles chiai* Teilhard de Chardin, 1940, *Lutra licenti* Teilhard de Chardin & Piveteau, 1930, *Casmaporthetes progressus* (Qiu, 1987), *Pachycrocuta licenti* (Pei, 1934), *Homotherium crenatidens* Fabrini, 1890, *Megantreon nihowanensis* (Teilhard de Chardin & Piveteau, 1930), *Sivapentahera* cf. *S. pleistocaenicus* (Zdansky, 1925), *Lynx shansius* Teilhard de Chardin, 1945, *Hipparion* (*Proboscidipparion*) *sinense* (Sefve, 1927), *Equus sanmeniensis* Teilhard de Chardin & Piveteau, 1930, *Coelodonta nihowanensis* Kahlke, 1969, *Muntiacus bohlini* (Teilhard de Chardin, 1940), *Eucladoceros boulei* Teilhard de Chard & Piveteau, 1930, *Nipponicervus elegans* (Teilhard de Chardin & Piveteau, 1930), *Elaphurus bifurcates* Teilhard de Chardin & Piveteau, 1930, *Spirocerus wongi* Teilhard de Chardin & Piveteau, 1930, *Gazella sinensis* Teilhard de Chardin & Piveteau, 1930, and *Bison palaeosinensis* Teilhard de Chardin & Piveteau, 1930; and 3) a considerable number of Middle to Late Pleistocene and extant species, such as *Canis* sp. (Majuangou), *Vulpes* sp. (Danangou), *Martes* sp. (Xiaochangliang), *Ursus thibetanus* G. Cuvier, 1823, *Viverra* sp. (Xiaochangliang), *Felis* sp. (Nihewan Village), *Sus* cf. *S. lydekkeri* Zdansky, 1928, *Axis* sp. (Danangou), *Cervus* sp. (Nihewan Village, Xiaochangliang), *Gazella* sp. (Xiaochangliang), *Gazella* cf. *G. subgutturosa* (Güldenstädt, 1780), *Ovis* sp. (Nihewan Village), *Ovis shantungensis* Matsumoto, 1926, *Bison* sp. (Xiaochangliang), and so on.

Acknowledgements This work was supported by the Strategic Priority Research Program of Chinese Academy of Sciences (Grant No: XDB26000000) and National Science Foundation of China (Grant No: 41772018). Prof. YAO Pei-Yi and Prof. YAO Zhen of Institute of Geology, Chinese Academy of Geological Sciences, Mr. CHEN Xing-Qiang of China University of Geosciences participated in the field investigation and fossil collection. Mr. WANG Zhao of Institute of Vertebrate Paleontology and Paleoanthropology, Chinese Academy of Sciences (IVPP) participated in the excavation and prepared the fossils. Mr. GAO Wei of IVPP photographed the specimens. Prof. QIU Zhang-Xiang of IVPP gave valuable comments and suggestions during the preparation of the manuscript. Prof. ZHANG Zhao-Qun and Prof. LI Qiang of IVPP provided helpful comments that improved the content of the article when reviewing the manuscript. We would like to express our profound gratitude to these institutions and individuals.

泥河湾盆地叶沟晚上新世贺风三趾马动物群及其生物地层学意义

刘金毅[1,2] 张颖奇[1,2] 迟振卿[3] 王 永[3] 杨劲松[4] 郑绍华[1]

(1 中国科学院古脊椎动物与古人类研究所，中国科学院脊椎动物演化与人类起源重点实验室 北京 100044)

(2 中国科学院生物演化与环境卓越创新中心 北京 100044)

(3 中国地质科学院地质研究所 北京 100037)

(4 中国地质科学院水文地质环境地质研究所 石家庄 050061)

摘要：目前对于泥河湾盆地晚新生代地层的年代学认识还存在分歧，基于哺乳动物化石的生物地层学对比结果与基于磁性地层学的年代测定结果存在较大矛盾。生物地层学对比表明，泥河湾盆地桑干河峡谷地带与壶流河下游两岸出露的风成红粘土、含砂砾石河湖相红粘土与沼泽相砂质粘土属上上新统；而磁性地层学研究一般将其归为下更新统。记述了泥河湾盆地叶沟晚上新世贺风三趾马动物群，由丁氏貉*Nyctereutes tingi*, 中华貉*N. sinensis*, 比利牛斯硕鬣狗*Pachycrocuta pyrenaica*, 锯齿虎属(未定种) *Homotherium* sp., 贺风(近)三趾马*Hipparion* (*Plesiohipparion*) *houfenense*, 额鼻角犀属(未定种) *Dicerorhinus* sp., 麂属(未定种) *Muntiacus* sp., 山西轴鹿*Axis shansius*, 步氏羚羊*Gazella blacki*, 副驼属(未定种) *Paracamelus* sp.等9属10种构成。这个动物群的组成与经典的泥河湾早更新世动物群显著不同，是泥河湾盆地内上上新统存在的新证据。在系统记述的基础上，对叶沟贺风三趾马动物群的时代和组成进行了讨论，并对泥河湾盆地晚上新世与早更新世大型哺乳动物群的组合特征进行了归纳，以期对今后泥河湾盆地的地层学研究工作有所帮助。

关键词：泥河湾盆地，上上新统，大型哺乳动物，贺风三趾马，生物地层学，磁性地层学

References

Adrover R, Morales J, Soria D, 1976. Hallazgo de *Hyaena donnezani* Viret en La Calera II (Aldehuela, provincia de Teruel). Teruel, 55-56: 189–205

Allen G M, 1938. The mammals of China and Mongolia, Part 1. New York: The American Museum of Natural History. 1–620

Anton M, Salesa M J, Morales J et al., 2004. First known complete skulls of the scimitar-toothed cat *Machairodus aphanistus* (Felidae, Carnivora) from the Spanish Late Miocene site of Batalones–1. J Vert Paleont, 24(4): 957–969

Ao H, An Z S, Dekkers M J et al., 2013. Pleistocene magnetochronology of the fauna and Paleolithic sites in the Nihewan Basin: significance for environmental and hominin evolution in North China. Quat Geochronol, 18: 78–92

Ballesio R, 1963. Monographie d'un *Machairodus* du gisement villafranchien de Senèze: *Homotherium crenatidens* Fabrini. Trav Doc Lab Géol Lyon, N Sér, 9: 1–129

Cai B Q, Li Q, 2004. Human remains and the environment of Early Pleistocene in the Nihewan Basin. Sci China, Ser D-Earth Sci, 47(5): 437–444

Cai B Q, Zhang Z Q, Zheng S H et al., 2004. New advances in the stratigraphic study on representative sections in the Nihewan Basin, Hebei. Prof Pap Stratigr Palaeont, 28: 267–285

Cai B Q, Li Q, Zheng S H, 2008. Fossil mammals from Majuangou section of Nihewan Basin, China and their age. Acta Anthrop Sin, 27(2): 127–140

Cai B Q, Zheng S H, Liddicoat J C et al., 2013. Review of the litho-, bio-, and chronostratigraphy in the Nihewan Basin, Hebei, China. In: Wang X M, Flynn L J, Fortelius M eds. Fossil mammals of Asia – Neogene Biostratigraphy and Chronology. New York: Columbia University Press. 218–242

Chen C, Shen C, Chen W Y et al., 1999. 1998 excavation of the Xiaochangliang site at Yangyuan, Hebei. Acta Anthrop Sin, 18(3): 225–239

Chen G F, 1997a. *Gazella blacki* Teilhard and Young, 1931 (Bovidae, Artidactyla, Mammalia) from the Late Pliocene of Hefeng, Jingle District, Shanxi Province. Vert PalAsiat, 35(3): 189–200

Chen G F, 1997b. The genus *Gazella* Blainville, 1861 (Bovidae, Artiodactyla) from the Late Neogene of Yushe Basin, Shanxi Province, China. Vert PalAsiat, 35(4): 233–249

Chen X F, 1994. Stratigraphy and large mammals of the "Jinglean" Stage, Shanxi, China. Quaternary Sci, 14(4): 339–353

Chia L P, Wang C, 1978. Hsihoutu – a culture site of Early Pleistocene in Shansi Province. Beijing: Cultural Relics Publishing House. 1–85

Croizet J B, Jobert A, 1828. Recherches sur les ossements fossils du département du Puy-de-Dôme. Clermont-Ferrand: Thibaud-Landriot édit. 1–224

Crusafont M, Sondaar P, 1971. Une nouvelle espèce d'*Hipparion* du Miocène terminal d'Espagne. Palaeovertebrata, 4(2): 59–66

Daguenet T, Sen S, 2019. Phylogenetic relationships of *Nyctereutes* Temminck, 1838 (Canidae, Carnivora, Mammalia) from Early Pliocene of Çalta, Turkey. In: de Bonis L, Werdelin L eds. Memorial to Stéphane Peigné: Carnivores (Hyaenodonta and Carnivora) of the Cenozoic. Geodiversitas, 41(18): 663–677

de Beaumont G, 1975. Recherches sur les Félidés (Mammifères, Carnivores) du Pliocène inférieur des sables à *Dinotherium* des environs d'Eppelsheim (Rheinhessen). Arch Sci, 28(3): 369–405

de Beaumont G, 1978. Notes complémentaires sur quelques Félidés (Carnivores). Arch Sci, 31(3): 219–227

Deng C L, 2011. Chapter 2, Section 4, Chronology of magnetic stratigraphy. In: Yuan B Y, Xia Z K, Niu P S eds. Nihewan Rift and Early Man. Beijing: Geological Publishing House. 61–68

Deng C L, Zhu R X, Zhang R et al., 2008. Timing of the Niheawan formation and faunas. Quaternary Res, 69(1): 77–90

Deng T, Hou S K, 2011. The Mazegouan Stage of the continental Pliocene Series in China. J Stratigr, 35(3): 237–249

Deng T, Zheng M, 2005. Limb bones of *Elasmotherium* (Rhinocerotidae, Perissodactyla) from Nihewan (Hebei, China). Vert PalAsiat, 43(2): 110–121

Deng T, Hou S K, Wang T M et al., 2010. The Gaozhuangian Stage of the continental Pliocene series in China. J Stratigr, 34(3): 225–240

Depéret C, 1890. Les animaux Pliocènes du Roussillon. Mém Soc Géol Fr, Paléont, 3: 1–164

Du H J, Wang A D, Zhao Q Q et al., 1988. On a new stratigraphic unit – Daodi Formation of Late Pliocene of Nihewan Basin. Earth Sci-J China Univ Geosci, 13(5): 561–568

Farjand A, Zhang Z Q, Liu W H et al., 2021. The evolution of *Nyctereutes* (Carnivora: Canidae) in the Nihewan Basin, Hebei, northern China. Palaeoworld, 30(2): 373–381

Fejfar O, 1964. The lower-Villafrancian vertebrates from Hajnáčka near Filákovo in southern Slovakia. Rozpr Ústředn Ústavu Geol, 30: 1–115

Ficcarelli G, 1979. The Villafranchian machairodonts of Tuscany. Palaentogr Ital, 71(N S 41): 17–26

Flynn L J, Qiu Z X, 2013. Biostratigraphy and the Yushe Basin. In: Tedford R H, Qiu Z X, Flynn L J eds. Late Cenozoic Yushe Basin, Shanxi Province, China: Geology and Fossil Mammals, Vol. I: History, Geology, and Magnetostratigraphy. New York: Springer. 79–82

Flynn L J, Tedford R H, Qiu Z X, 1991. Enrichment and stability in the Pliocene mammalian fauna of North China. Paleobiology, 17(3): 246–265

Howell F C, Petter G, 1980. The *Pachycrocuta* and *Hyaena* lineages (Plio-Pleistocene and extant species of the Hyaenidae) – their relationships with Miocene ictiteres: *Palhyaena* and *Hyaenictitherium*. Geobios, 13(4): 579–623

Huang W B, Zhong Z K, 1991. Chapter 6, Section 1, Carnivora Bowdich, 1821. In: Huang W B, Fang Q R et al. eds. Wushan Hominid Site. Beijing: China Ocean Press. 92–112

Huang W B, Tang Y J, Zong G F et al., 1974. Observation of several Late Cenozoic stratigraphic sections in the Nihewan Basin. Vert PalAsiat, 12(2): 99–108

Huang W B, Zheng S H, Zong G F et al., 1993. Pliocene mammals from the Leijiahe Formation of Lingtai, Gansu, China – Preliminary report on field work in 1972 and 1992. North Hemisph Geo-Bio Trav, 1: 29–37

Jen P H, 1965. Mammalian fossils from an Upper Cenozoic section at Puchen, Shensi. Vert PalAsiat, 9(3): 298–301

Kurtén B, Anderson E, 1980. Pleistocene Mammals of North America. New York: Columbia University Press. 1–398

Li Q, Zheng S H, Cai B Q, 2008. Pliocene biostratigraphic sequence in the Nihewan Basin, Hebei, China. Vert PalAsiat, 46(3): 210–232

Li Y, 1984. The Early Pleistocene mammalian fossils of Danangou, Yuxian, Hebei. Vert PalAsiat, 22(1): 60–68

Liu J Y, 2003. Machairondont and other carnivore fossils from the Renzidong Cave, Fanchang County, Anhui Province, China. Ph. D. Dissertation. Beijing: Graduate School of Chinese Academy of Sciences. 1–257

Liu J Y, Qiu Z X, 2009. Chater 4, Section 6, Carnivora. In: Jin C Z, Liu J Y eds. Paleolithic Site – The Renzidong Cave, Fanchang, Anhui Province. Beijing: Science Press. 220–283

Liu J Y, Fang Y S, Zhang Z H, 2007. Chapter 2, Section 2, Carnivora Bowdich, 1821. In: Nanjing Museum, Institute of Archaeology, Jiangsu Province eds. The Early Pleistocene Mammalian Fauna at Tuozi Cave, Nanjing, China. Beijing: Science Press. 25–68

Liu P, Qin H F, Li S H et al., 2021. Magnetostratigraphic dating of the Danangou and Dongyaozitou mammalian faunas in the Nihewan Basin, North China. Quaternary Sci Rev, 257: 106855

Liu W H, 2019. *Nyctereutes* from Hongya Yangshuizhan Locality at Nihewan Basin, and the systematic revision of the genus *Nyctereutes*. PhD Dissertation. Beijing: University of Chinese Academy of Sciences. 1–353

Pei W C, 1934. On the Carnivores from Locality 1 of Choukoutien. Palaeont Sin, Ser C, 8: 1–166

Qiu Z X, 1987. Die Hyaeniden aus dem Ruscinium und Villafranchium Chinas. Münchner Geowiss Abh Reihe A, Geol Paläont, 9: 1–108

Qiu Z X, 2000. Nihewan fauna and Q/N boundary in China. Quaternary Sci, 20(2): 142–154

Qiu Z X, Huang W L, Kuo Z H, 1980. Notes on the first discovery of the skull of *Hipparion houfenense*. Vert PalAsiat, 18(2): 131–137

Qiu Z X, Huang W L, Guo Z H, 1987. The Chinese hipparionine fossils. Palaeont Sin, New Ser C, 25: 1–250

Qiu Z X, Deng T, Wang B Y, 2004. Early Pleistocene mammalian fauna from Longdan, Dongxiang, Gansu, China. Palaeont Sin, New Ser C, 27: 1–198

Qiu Z X, Shi Q Q, Liu J Y, 2008. Description of skull material of *Machairodus horribilis* Schlosser, 1903. Vert PalAsiat, 46(4): 265–283

Repenning C A, Fejfar O, Heinrich W -D, 1990. Arvicolid rodent biochronology of the Northern Hemisphere. In: Fejfar O, Heinrich W -D eds. International Symposium – Evolution, Phylogeny and Biostratigraphy of Arvicolids (Rodentia, Mammalia). Prague: Geological Survey. 385–418

Schütt G, 1972. Fossil mammals of Java. IV. On Pleistocene hyenas of Java. Proc K Ned Akad Wet, Ser B, 75(4): 261–288

Sharapov S, 1989. On a new species of the saber-toothed cat from the Late Eopleistocene of Afgano-Tadjik depression and the evolution of the genus *Homotherium Fabrini*, 1890. Paleont Zh, 3: 73–83

Soria D, Aguirre E, 1976. El cánido de Layna: revisión de los *Nyctereutes* fósiles. Trab Neóg Cuat, 5: 83–115

Sotnikova M V, 1992. A new species of *Machairodus* from the Late Miocene Kalmakpai locality in eastern Kazakhstan (USSR). Ann Zool Fenn, 28(3-4): 361–369

Sun D H, Chen M Y, Shaw J et al., 1998. Magnetostratigraphy and palaeoclimatic records of the Late Cenozoic aeolian dust accumulation sequences from China Loess Plateau. Sci China, Ser D, 28(1): 79–84

Tang Y J, 1980a. Early Pleistocene stratigraphy and mammalian fossils from Wenxi, southwestern Shansi. Vert PalAsiat, 18(1): 33–44

Tang Y J, 1980b. Note on a small collection of Early Pleistocene mammalian fossils from northern Hebei. Vert PalAsiat, 18(4): 314–323

Tang Y J, Ji H X, 1983. A Pliocene-Pleistocene transitional fauna from Yuxian, northern Hebei. Vert PalAsiat, 21(3): 245–254

Tang Y J, You Y Z, Li Y, 1981. Some new fossil localities of Early Pleistocene from Yangyuan and Yuxian basins, northern Hopei. Vert PalAsiat, 19(3): 256–268

Tang Y J, Li Y, Chen W Y, 1995. Mammalian fossils and the age of Xiaochangliang Paleolithic site of Yangyuan, Hebei. Vert PalAsiat, 33(1): 74–83

Tedford R H, Qiu Z X, 1991. Pliocene *Nyctereutes* (Carnivora: Canidae) from Yushe, Shanxi, with comments on Chinese fossil racoon-dogs. Vert PalAsiat, 29(3): 176–189

Tedford R H, Taylor B E, Wang X M, 1995. Phylogeny of the Caninae (Carnivora: Canidae): the living taxa. Am Mus Novit, 3146: 1–37

Tedford R H, Wang X M, Taylor B E, 2009. Phylogenetic systematics of the North American fossil Caninae (Carnivora: Canidae). Bull Am Mus Nat Hist, 325: 1–218

Teilhard de Chardin P, Leroy P, 1945. Les Félidés de Chine. Publ Inst Géo-Biol, Pékin, 11: 1–58

Teilhard de Chardin P, Pei W C, 1941. The fossil mammals from Locality 13 of Choukoutien. Palaeont Sin, Ser C, 11: 1–106

Teilhard de Chardin P, Piveteau J, 1930. Les mammifères fossils de Nihowan (Chine). Ann Paléont, 19: 1–134

Teilhard de Chardin P, Trassaert M, 1937. Pliocene Camelidae, Graffidae and Cervidae of south-eastern Shansi. Palaeont Sin, New Ser C, 1: 1–68

Teilhard de Chardin P, Young C C, 1931. Fossil mammals from the Late Cenozoic of northern China. Palaeont Sin, Ser C, 9(1): 1–88

Tong H W, Wang F G, Zheng M et al., 2014. New fossils of *Stephanorhinus kirchbergensis* and *Elasmotherium peii* from the Nihewan Basin. Acta Anthrop Sin, 33(3): 369–388

Tong Y S, Huang W B, Qiu Z D, 1975. A *Hipparion* fauna from Anle, Huoxian, Shanxi. Vert PalAsiat, 13(1): 34–47

Tseng Z J, Wang X M, Li Q et al., 2016. Pliocene bone-cracking Hyaeninae (Carnivora, Mammalia) from the Zanda Basin, Tibet Autonomous Region, China, Hist Biol, 28(1-2): 69–77, doi: 10.1080/08912963.2015.1004330

Turner A, Antón M, Werdelin L, 2008. Taxonomy and evolutionary patterns in the fossil Hyaenidae of Europe. Geobios, 41(5): 677–687

Viret M J, 1954. Le loess a bancs durcis de Saint-Vailler (Drôme), et sa faune de mammifères Villafranchiens. Nouv Arch Mus Hist Nat Lyon, 4: 1–200

Wang A D, 1982. The discovery of Pliocene mammals from Nihewan area and its significance. Kexue Tongbao (Chinese Sci Bull), 27(9): 990–993

Wang X M, Grohé G, Su D F et al., 2017. A new otter of giant size, *Siamogale melilutra* sp. nov. (Lutrinae: Mustelidae: Carnivora), from the latest Miocene Shuitangba site in north-eastern Yunnan, south-western China, and a total-evidence phylogeny of lutrines. J Syst Palaeont, 16(1): 39–65

Wei G B, Taruno H, Jin C Z et al., 2003. The earliest specimens of the steppe mammoth, *Mammuthus trogontherii*, from the Early Pleistocene Nihewan Formation, North China. Earth Sci (Chikyu Kagaku), 57: 289–298

Weithofer K A, 1889. Die fossilen Hyänen des Arnotales in Toskana. Denk Kaiser Akad Wiss, Math-Naturwiss Classe, 55: 337–360

Werdelin L, Solounias N, 1991. The Hyaenidae: taxonomy, systematics and evolution. Fossils Strata, 30: 1–104

Xue X X, 1981. An Early Pleistocene mammalian fauna and its stratigraphy of the River You, Weinan, Shensi. Vert PalAsiat, 19(1): 35–44

You Y Z, Tang Y J, Li Y, 1980. Discovery of Paleolithic stone artifacts from the Nihewan Formation. Quaternary Sci, 5(1): 1–11

Young C C, 1932. On the Artiodyctyla from the *Sinanthropus* Site at Choukoutien. Palaeont Sin, Ser C, 8(2): 1–158

Zdansky O, 1924. Jungteriare Carnivoren Chinas. Palaeont Sin, Ser C, 2 (1): 1–149

Zdansky O, 1926. *Paracamelus gigas*, Schlosser. Palaeont Sin, Ser C, 2(4): 1–44

Zhang et al., 1993. Comprehensive study on the Jinniushan Paleolithic Site. Mem Inst Vert Palaeont Palaeoanthrop, Acad Sin, 19: 1–163

Zhang Y Q, Kawamura Y, Cai B Q, 2008. Small mammal fauna of Early Pleistocene age from the Xiaochangliang site in the Nihewan Basin, Hebei, nortern China. Quaternary Res, 47(2): 81–92

Zhang Y X, Sun D H, An Z S et al., 1999. Mammalian fossils from Late Pliocene (lower MN 16) of Lingtai, Gansu Province. Vert PalAsiat, 37(3): 190–199

Zhang Z Q, 2001. Fossil mammals of Early Pleistocene from Ningyang, Shandong Province. Vert PalAsiat, 39(2): 139–150

Zhang Z Q, Zheng S H, Liu J B, 2003. Pliocene micromammalian biostratigraphy of Nihewan Basin, with comments on the stratigraphic division. Vert PalAsiat, 41(4): 306–313

Zheng S H, Cai B Q, 1991. Micromammalian fossils from Danangou of Yuxian, Hebei. In: Institute of Vertebrate Paleontology and Paleoanthropology, Academia Sinica ed. Contributions to the XIII INQUA. Beijing: Beijing Scientific and Technological Publishing House. 100–131

Zheng S H, Wu W Y, Li Y et al., 1985. Late Cenozoic mammalian faunas of Guide and Gonghe basins, Qinghai Province. Vert PalAsiat, 23(2): 89–134

Zhou X Y, 1988. The Pliocene micromammalian fauna from Jingle, Shanxi – a discussion of the age of Jingle Red Clay. Vert PalAsiat, 26(3): 181–197

Zhu R X, Deng C L, Pan Y X, 2007. Magnetochronology of the fluvio-lacustrine sequences in the Nihewan Basin and its implications for early human colonization of northeast Asia. Quaternary Sci, 27(6): 922–944

Zong G F, Tang Y J, Xu Q Q et al., 1982. The Early Pleistocene in Tunliu, Shanxi. Vert PalAsiat, 20(3): 236–247